



## OPEN ACCESS

## EDITED BY

John Maher,  
King's College London, United Kingdom

## REVIEWED BY

Caroline Hull,  
Leucid Bio, United Kingdom  
Haeyoun Choi,  
Catholic University of Korea,  
Republic of Korea

## \*CORRESPONDENCE

Tamara Verkerk  
✉ t.verkerk@sanquin.nl  
S. Marieke van Ham  
✉ m.vanham@sanquin.nl

RECEIVED 11 November 2023

ACCEPTED 01 February 2024

PUBLISHED 15 February 2024

## CITATION

Verkerk T, Pappot AT, Jorritsma T, King LA,  
Duurland MC, Spaapen RM and van Ham SM  
(2024) Isolation and expansion of pure and  
functional  $\gamma\delta$  T cells.  
*Front. Immunol.* 15:1336870.  
doi: 10.3389/fimmu.2024.1336870

## COPYRIGHT

© 2024 Verkerk, Pappot, Jorritsma, King,  
Duurland, Spaapen and van Ham. This is an  
open-access article distributed under the terms  
of the [Creative Commons Attribution License  
\(CC BY\)](https://creativecommons.org/licenses/by/4.0/). The use, distribution or reproduction  
in other forums is permitted, provided the  
original author(s) and the copyright owner(s)  
are credited and that the original publication  
in this journal is cited, in accordance with  
accepted academic practice. No use,  
distribution or reproduction is permitted  
which does not comply with these terms.

# Isolation and expansion of pure and functional $\gamma\delta$ T cells

Tamara Verkerk<sup>1,2,3\*</sup>, Anouk T. Pappot<sup>1,2</sup>, Tineke Jorritsma<sup>1</sup>,  
Lisa A. King<sup>3,4,5</sup>, Mariël C. Duurland<sup>1</sup>, Robbert M. Spaapen<sup>1,2</sup>  
and S. Marieke van Ham<sup>1,2,6\*</sup>

<sup>1</sup>Department of Immunopathology, Sanquin Research, Amsterdam, Netherlands, <sup>2</sup>Landsteiner Laboratory, Amsterdam UMC, University of Amsterdam, Amsterdam, Netherlands, <sup>3</sup>Amsterdam Institute for Infection and Immunity, Amsterdam, Netherlands, <sup>4</sup>Department of Medical Oncology, Amsterdam UMC, Vrije Universiteit Amsterdam, Amsterdam, Netherlands, <sup>5</sup>Cancer Center Amsterdam, Amsterdam, Netherlands, <sup>6</sup>Swammerdam Institute for Life Sciences, University of Amsterdam, Amsterdam, Netherlands

$\gamma\delta$  T cells are important components of the immune system due to their ability to elicit a fast and strong response against infected and transformed cells. Because they can specifically and effectively kill target cells in an MHC independent fashion, there is great interest to utilize these cells in anti-tumor therapies where antigen presentation may be hampered. Since only a small fraction of T cells in the blood or tumor tissue are  $\gamma\delta$  T cells, they require extensive expansion to allow for fundamental, preclinical and *ex vivo* research. Although expansion protocols can be successful, most are based on depletion of other cell types rather than  $\gamma\delta$  T cell specific isolation, resulting in unpredictable purity of the isolated fraction. Moreover, the primary focus only lies with expansion of  $V\delta 2^+$  T cells, while  $V\delta 1^+$  T cells likewise have anti-tumor potential. Here, we investigated whether  $\gamma\delta$  T cells directly isolated from blood could be efficiently expanded while maintaining function.  $\gamma\delta$  T cell subsets were isolated using MACS separation, followed by FACS sorting, yielding >99% pure  $\gamma\delta$  T cells. Isolated  $V\delta 1^+$  and  $V\delta 2^+$  T cells could effectively expand immediately after isolation or upon freeze/thawing and reached expansion ratios between 200 to 2000-fold starting from varying numbers using cytokine supported feeder stimulations. MACS/FACS isolated and PHA stimulated  $\gamma\delta$  T cells expanded as good as immobilized antibody mediated stimulated cells in PBMCs, but delivered purer cells. After expansion, potential effector functions of  $\gamma\delta$  T cells were demonstrated by IFN- $\gamma$ , TNF- $\alpha$  and granzyme B production upon PMA/ionomycin stimulation and effective killing capacity of multiple tumor cell lines was confirmed in killing assays. In conclusion, pure  $\gamma\delta$  T cells can productively be expanded while maintaining their anti-tumor effector functions against tumor cells. Moreover,  $\gamma\delta$  T cells could be expanded from low starting numbers suggesting that this protocol may even allow for expansion of cells extracted from tumor biopsies.

## KEYWORDS

gamma delta ( $\gamma\delta$ ) T cells, isolation and expansion, functional validation, method comparison, high purity

## Introduction

$\gamma\delta$  T cells are considered to be potent cells to combat infections and malignancies because of their strategic localization in mucosal tissues, specific recognition of target cells and direct response upon activation. Like  $\alpha\beta$  T cells,  $\gamma\delta$  T cells have a potent capacity to elicit a cytotoxic response upon specific activation via release of TNF- $\alpha$ , IFN- $\gamma$ , perforins and granzymes (1–3). Unlike  $\alpha\beta$  TCRs,  $\gamma\delta$ -TCR triggering is typically independent of antigens presented on major histocompatibility complex I or II (MHC-I/II). In addition,  $\gamma\delta$  T cells are fully mature when they leave the thymus, have a broad range of antigen recognition and can consequently respond rapidly to antigen encounter. Similar to both  $\alpha\beta$  T cells and natural killer (NK) cells,  $\gamma\delta$  T cells express NKG2D which can detect stress-induced signals on tumors and infected cells (4). In addition, these cells also share other receptors with innate NK cells such as Fc $\gamma$ RIIIa (CD16) which is required to recognize opsonized tumor cells, DNAX accessory molecule (DNAM-1, CD226) and natural cytotoxicity receptors (NCRs) NKp46, NKp44 and NKp30 which promote anti-tumor cytotoxicity (5, 6).

$\gamma\delta$  T cells can be divided into different subsets based on the composition of the TCR chains of which V $\delta$ 1 and V $\delta$ 2 are two major  $\gamma\delta$  T cells subsets found in humans. Both types can be found in peripheral blood of which the majority are V $\delta$ 2 T cells. V $\delta$ 1 T cells mainly reside in tissues and mucosa, such as the skin, spleen, gut, and lungs (7–10).

The majority of  $\gamma\delta$  T cells are activated in an MHC-I independent manner and only a few  $\gamma\delta$  T cell clones have been reported to become activated by classical MHC-I molecules (11–13). V $\delta$ 1 T cells recognize MICA/B and ULBPs on cells through  $\gamma\delta$  TCR and NKG2D engagement or CD1c/d on antigen presenting cells (1, 14). V $\delta$ 2 T cells harbor a TCR that can be activated through surface expression of the butyrophilin (BTN) BTN3A1/BTN2A1 complex, modulated by pathogenic changes in cells (15, 16). Accumulation of intracellular phosphoantigens (pAgs) instigates a conformational change of the BTN complex, via pAgs binding to the intracellular BTN3A1 B30.2 domain, which is important for V $\delta$ 2 T cell activation (15, 17).

The mode of action of  $\gamma\delta$  T cells in an anti-tumor response comprises direct cytolytic activity via NKG2D, Fc $\gamma$ RIII, Fas/Fas-ligand, DNAM-1 receptor-ligand interaction and the TNF related apoptosis inducing ligand (TRAIL) pathway resulting in production of perforins, granzymes, IFN- $\gamma$  and TNF- $\alpha$  (4, 5, 18–23). In concurrence,  $\gamma\delta$  T cells can also activate other immune cells (24, 25), for instance activate NK cells via co-stimulation, promote dendritic cell (DC) maturation and support initiation of a humoral immune response (26–31).

Interestingly, V $\delta$ 1 and V $\delta$ 2 T cell subsets can represent up to 50% of CD3<sup>+</sup> tumor infiltrating lymphocytes (TILs), although this varies between tumor type and stage (1, 32–36). Recently, Knight and colleagues found increased frequencies of both V $\delta$ 1 and V $\delta$ 2 T cells in patients with chronic myeloid leukemia (CML) compared to age-matched healthy donors and demonstrated primary CML specific lysis by autologous V $\delta$ 1 T cells (35). Some studies found correlations between tumor infiltrating  $\gamma\delta$  T cells with a favorable clinical outcome. For example, the study conducted by Gentles and

co-authors found that intra-tumoral signatures of  $\gamma\delta$  T cells were the most significant, favorable anti-tumor prognostic factor by analyzing leukocyte frequencies of 22 cell types from 25 pooled human cancers (37). It remains to be established though if tumor infiltrating  $\gamma\delta$  T cells can be used as a prognostic factor (1, 25, 33, 38, 39). Motivation for the application of  $\gamma\delta$  T cells in immunotherapy is driven by the distinctive MHC independent activation, meaning that its application is not restricted to an autologous setting. In addition, they have a potential to be used for tumors showing immune escape through downmodulation of MHC expression. Immunotherapy based on  $\gamma\delta$  T cells involves *in vivo* stimulation of V $\delta$ 2 T cells through intravenous administration of pamidronate or zoledronate, which are bisphosphonates stimulating the conformational change of the BTN3A1/BTN2A1 complex, and autologous or allogenic reinfusion of *ex vivo* zoledronate driven expanded  $\gamma\delta$  T cells (3, 15, 40–42). These treatments have been shown to have minor adverse effects and to be effective for a number of patients suffering from for example, pancreatic, lung, liver and hematological cancers, especially in combination with other conventional therapies (3, 40, 43–53).

The low number of  $\gamma\delta$  T cells in peripheral blood (0.5–5% of T cells) and, especially, in tumor tissue represents a major challenge for their application in fundamental, preclinical and *ex vivo* studies (54–56). Therefore, expansion of  $\gamma\delta$  T cells is often applied to study these cells.

Scientific reports in which expanded  $\gamma\delta$  T cells are used are mainly subset specific and vary in isolation and expansion strategies. Most used methods are based on the use of bisphosphonates zoledronate, pamidronate or bromohydrin pyrophosphate (BrHPP) to activate V $\delta$ 2 T cells specifically residing in total PBMCs (49, 57–59). These compounds inhibit the IPP processing enzyme farnesyl diphosphate synthase (FDPS), consequently increasing IPP levels and subsequent the BTN3A1/BTN2A1 structure (15). Zoledronate based expansion of V $\delta$ 2 T cells in total PBMCs can generate over 90% pure V $\delta$ 2 T cells, but shows strong variation in yields between donors (59–63). Other methods focus on TCR activation with, for instance, lectins such as phytohaemagglutinin (PHA) or anti-CD3 (OKT3) with or without anti-CD28 (64). In literature, TCR targeting activation methods are generally used to produce large numbers of V $\delta$ 1 T cells (65, 66). Other, less conventional methods have been described. For instance, Siegers and colleagues showed activation with the mitogen Concanavalin A can expand presorted V $\delta$ 1 and V $\delta$ 2  $\gamma\delta$  T cells (67). Lastly, K562 cells are used as feeder cells which are modified to express various molecules such as CD40L, CD70, CD80, CD86, CD83, CD137L and artificial membrane bound cytokines like IL-15 (58, 68, 69). Generally, IL-2 is used to promote activation, growth and proliferation, often combined with other cytokines like IL-4, IL-7, IL-15, IL-18 and IL-21 (58). Isolation of  $\gamma\delta$  T cells usually incorporates an  $\alpha\beta$  T cell depletion step, occasionally combined with an additional NK cell or undesired  $\gamma\delta$  subset depletion step, either before or after the expansion period.

The issues that accompany the current described methods is that they are variable, solely applicable to specific subsets and may yield unpredictable or impracticable levels purity of the (final) product. Hence, there is a need for a practical protocol that can

be used to specifically isolate V $\delta$ 1 and V $\delta$ 2 T cells followed by an expansion method that assures purity and maintains their functional properties. Standardized isolation and expansion protocols would allow for comparison between studies and benefit the growth of knowledge on  $\gamma\delta$  T cell differentiation, function and targets.

Here, we report an isolation and expansion method which reproducibly generates high and >99% pure V $\delta$ 1 and V $\delta$ 2 T cell numbers after 14 days of expansion using PBMC as starting material. This method focuses first on establishing  $\gamma\delta$  T cell populations through V $\delta$ 1 and V $\delta$ 2 T cell specific isolation, which can subsequently be expanded to over a 1000-fold increase. In addition, we show that these  $\gamma\delta$  T cells can effectively be activated and kill tumor cells. Moreover, this method can be used to expand cells from low starting numbers or frozen, previously expanded cells. Together, this allows investigators to reproducibly generate large batches of  $\gamma\delta$  T cells to study their biology.

## Materials and methods

### Isolation of $\gamma\delta$ T cells from PBMCs

Buffy coats were collected from healthy donors (Sanquin Blood Supply, Amsterdam, the Netherlands) who provided written informed consent for the use of their donation for research. Peripheral blood mononucleated cells (PBMCs) were isolated from buffy coats using Lymphoprep (Axis-Shield PoC AS, Dundee DD2 1XA, Scotland) density gradient. For direct targeted isolation of  $\gamma\delta$  T cells, PBMCs were incubated with PE conjugated mouse anti-human V $\delta$ 1 TCR or APC/PE conjugated mouse anti-human V $\delta$ 2 TCR for 30 minutes on ice (Table 1). For PAN  $\gamma\delta$  T cell isolation, unconjugated anti-PAN $\gamma\delta$  TCR was used (Table 1). The PBMCs were washed with PBS/0.1%BSA and incubated with anti-mouse IgG microbeads (Miltenyi) prior to positive MACS isolation according to manufacturer's protocol. Subsequently, the collected  $\gamma\delta$  T cells were purified using a FACS sort for PE<sup>+</sup> (V $\delta$ 1) or PE/APC<sup>+</sup> (V $\delta$ 2) cells. For PAN $\gamma\delta$  isolation, cells were stained with anti-IgG1 (APC) prior to FACS sort (Table 1). For untouched, pan  $\gamma\delta$  T cell isolation, the TCR $\gamma/\delta$ + T Cell Isolation Kit (Miltenyi) was used according to manufacturer's protocol. The purity of the isolated  $\gamma\delta$  T cells was assed prior to cell culture.

### Cell culture

The target cell lines WM9 and WiDr (kindly provided by prof. J.J. van der Vliet, Amsterdam UMC, the Netherlands) were cultured in DMEM (Gibco) supplemented with 10% FCS (Serana), antibiotics (PenStrep, Invitrogen), 1% L-glutamine (Gibco) and 0.05 mM BME (Sigma). The target cell line HAP1 and HT29 cell line, and the EBV-LCLs used as feeder cells were cultured in IMDM (Gibco) supplemented with 10% FCS and antibiotics. Freshly isolated, thawed or 14-day cultured  $\gamma\delta$  T cells were expanded using the protocol as described in this paper. In short,  $\gamma\delta$  T cells per well were expanded in IMDM containing feeder cells (0.1x10<sup>6</sup> irradiated

TABLE 1 Antibodies.

	Source	Identifier	Dilution
Mouse anti human IFN- $\gamma$ PE	Biolegend	502509	1:100
Mouse anti human TNF- $\alpha$ Pe-Cy7	BD	557647	1:100
Mouse anti human/mouse granzyme B BV421	Biolegend	396414	1:150
Mouse anti human BTN3A1/2/3	R&D systems, Biotechne	MAB7136	1:100
Mouse anti human PAN $\gamma\delta$ TCR	Beckman Coulter	IM1349	1:100
Mouse anti human V $\delta$ 1 TCR PE	eBioscience	12-5679-42	1:100
Mouse anti human V $\delta$ 1 TCR APC	Miltenyi	130-118-968	1:100
Mouse anti human V $\delta$ 2 TCR PE	Biolegend	331408	1:200
Mouse anti human V $\delta$ 2 TCR APC	Biolegend	331418	1:200
Mouse anti human CD3 BV510	BD	563109	1:200
Mouse anti human CD25 BV605	BD	562661	1:100
Mouse anti human CD27 PE-Cy7	Invitrogen	25-0279-42	1:200
Mouse anti human CD45RA PE	BD	555489	1:200
Mouse anti human CD69 BUV395	BD	564364	1:200
Mouse anti human CD137 BUV661	BD	741642	1:200
Goat anti mouse IgG1 AF633	ThermoFisher Scientific	A-21052	1:200

EBV-LCLs (50Gy) and 1x10<sup>6</sup> PBMCs (30Gy) per ml), 5% heat inactivated human serum (HS, Sanquin), 5% FCS and antibiotics supplemented with 120 U/mL IL-2 (Peprotech), 20 ng/mL IL-7 (Research grade, Miltenyi), 20 ng/mL IL-15 (Peprotech) and 1  $\mu$ g/mL Phytohaemagglutinin (PHA, HA16 Remel<sup>TM</sup>, Thermo Fisher Scientific) at the start of the culture. Cultures with 150 cells started in a 96-well plate in a total volume of 100  $\mu$ l, 15.000 cells started in a 48-well plate with a total volume of 500  $\mu$ l and cultures starting at 150.000 cells were performed in 24-well plates with a total volume of 1ml. Cell cultures were harvested, counted and replated in 24-well plates at day 7 and day 10 (15.000 and 150.000 start) or day 17 (150 start) to maintain these cytokine concentrations and a cell density of 0.5 x 10<sup>6</sup> cells per ml. All cells were cultured at 37°C and 5% CO<sub>2</sub>.

### Immobilized antibody mediated activation

Anti-PAN $\gamma\delta$  (IMMU510, Beckman Coulter), anti-V $\delta$ 1-PE and anti-V $\delta$ 2-PE (Table 1) were coated on tissue treated 24-well plates

at 1  $\mu\text{g/ml}$  in a total volume of 500  $\mu\text{l}$  PBS, overnight at 4°C. The PBS was removed and 1 million PBMCs were added in 1 ml of medium per well: IMDM containing 10% FCS, 5% HS, antibiotics supplemented with 120 U/ml IL-2, 20 ng/ml IL-7, 20 ng/ml IL-15. Cells were provided with additional medium, harvested, counted and replated as described. The cells were cultured at 37°C and 5% CO<sub>2</sub> for a 14-day period. After expansion,  $\alpha\beta$  T cells were depleted using a TCR $\alpha/\beta$  T cell depletion kit (Miltenyi) according to manufacturer's protocol. The percentage of V $\delta$ 1<sup>+</sup> T cells and V $\delta$ 2<sup>+</sup> T cells in the total PBMCs after isolation and after 14-days expansion was used to determine the absolute number of V $\delta$ 1<sup>+</sup> T cells and V $\delta$ 2<sup>+</sup> T cells. The fold expansion was calculated through division of the absolute number of V $\delta$ 1<sup>+</sup> T cells and V $\delta$ 2<sup>+</sup> T cells after expansion by the absolute starting numbers.

## PMA/Ionomycin stimulation

$\gamma\delta$  T cells were stimulated with 100 ng/ml PMA (Sigma-Aldrich) and 1  $\mu\text{g/ml}$  ionomycin (from *Streptomyces conglobatus*, Sigma-Aldrich) for 1.5 hours at 37°C and 5% CO<sub>2</sub>. Brefeldin A (1:1000, BD) was added to the medium at the start of stimulation for intracellular measurement of IFN- $\gamma$ , TNF- $\alpha$  and granzyme B. For analysis, the cells were transferred to a V-bottom plate and washed with cold PBS/0.5% BSA prior to staining. Production of IFN- $\gamma$ , TNF- $\alpha$  and granzyme B was measured using flow cytometry.

## Coculture assays

The target cells WM9, WiDr, HT29 and HAP1, were plated one day prior to the coculture with  $\gamma\delta$  T cells at a density of 15,000 cells/well in a flat-bottom 96-well plate and treated O/N with 10  $\mu\text{M}$  pamidronate (PAM, Sigma) in complete IMDM or DMEM. After the O/N culture, the wells were carefully washed to remove dead cells and freshly expanded  $\gamma\delta$  T cells were added at a 10:1 ratio (E:T) in a total volume of 100  $\mu\text{l}$  medium (IMDM). After a 5-hour coculture, the cells were harvested from the plates and transferred to V-bottom plates. Target cells that remained attached after the initial harvest were removed using trypsin and added to the V-bottom plate. The percentage of dead target cells and activation marker expression on  $\gamma\delta$  T cells were measured using flow cytometry.

## Flow cytometry

Antibodies used are listed in [Table 1](#).

PBMCs or  $\gamma\delta$  T cells were washed with PBS prior to staining. Extracellular staining was performed by incubation with specific antibodies and LIVE/DEAD NEAR-IR (1:1000, Thermo Fisher Scientific) diluted in PBS for 30 min. on ice in the dark. The cells were washed twice with buffer (PBS/0.5% BSA) and either resuspended in PBS and directly analyzed or fixated using the BD Cytotfix/Cytoperm fixation and permeabilization kit (BD Bioscience) according to the manufacturer's protocol. For

intracellular staining, cells were permeabilized and incubated with antibodies targeting IFN- $\gamma$ , TNF- $\alpha$  or granzyme B diluted in permeabilization buffer for 30 min. on ice. Subsequently, the cells were washed twice and resuspended in PBS prior to analysis. To assess BTN3A1/2/3 levels on target cells, the cells were incubated with NEAR-IR and anti-BTN3A1/2/3 for 30 min. on ice. Next, the cells were washed twice with PBS and incubated with anti-IgG1 for 30 min on ice, followed by another two wash steps and resuspended in PBS prior to analysis. Stained cells were analyzed or sorted on BD flow cytometers (LSR-II, Fortessa, FACSymphony or ARIA-II) and analyzed using FlowJo™ software version 10.9.0 (Ashland, OR: Becton, Dickinson and Company; 2023).

For analysis of  $\gamma\delta$  T cells in PBMCs, after isolation and stimulation, the cells were gated on single cells, time, NEAR-IR negative events and CD3, V $\delta$ 1 or V $\delta$ 2 positive events. For analysis of target cell killing,  $\gamma\delta$  T cell were distinguished using the gating strategy as described and remaining cells were gated for single cells and time before NEAR-IR evaluation representing dead cells.

## Statistical analysis

Statistical testing was done by a student's T-test or a one-way ANOVA followed by a Tukey's multiple comparison test and are indicated in the figure legends. The statistical analysis was performed using GraphPad Prism version 10.0 for Mac OS (GraphPad Software, Boston, Massachusetts USA). Differences were considered significant when  $p \leq 0.05$ .

## Results

### V $\delta$ 2 T cells directly isolated from PBMCs can reach a 734-fold expansion on average during a 14-day culture period

V $\delta$ 2 T cells are the most prevalent  $\gamma\delta$  subset in the peripheral blood. To examine if V $\delta$ 2 T cells can be efficiently isolated directly from PBMCs and subsequently expanded, magnetic isolation was performed using mouse anti-V $\delta$ 2 TCR antibodies and anti-mouse IgG beads (MACS), followed by a FACS sort. MACS isolation generally yielded between 80-90% pure V $\delta$ 2<sup>+</sup> T cells (of living cells) which could be improved to >99% with FACS sort ([Figure 1A](#); [Supplementary Figure 1A](#)).

Culture of the cells was initiated at either 15,000 or 150,000 cells per well to determine the effect of cell seeding density on expansion. During expansion, the percentage of V $\delta$ 2<sup>+</sup> T cells remained stable with a >98% purity with a minor reduction to approx. 95% at day ([Figure 1B](#); [Supplementary Figures 1A, B](#)). Cultures which started with 15,000 cells reached cell numbers of 3.3-38.5 million cells at day 14 and cultures starting with 150,000 cells resulted in 33.9-39.5 million cells after 14 days ([Figure 1C](#)). There was no significant difference in expansion between the different seeding densities (15,000 versus 150,000 cells) ([Figure 1C](#)). Direct isolation targeting the V $\delta$ 2 TCR thus yields pure V $\delta$ 2<sup>+</sup> T cells populations (>99%) which can successfully be expanded.

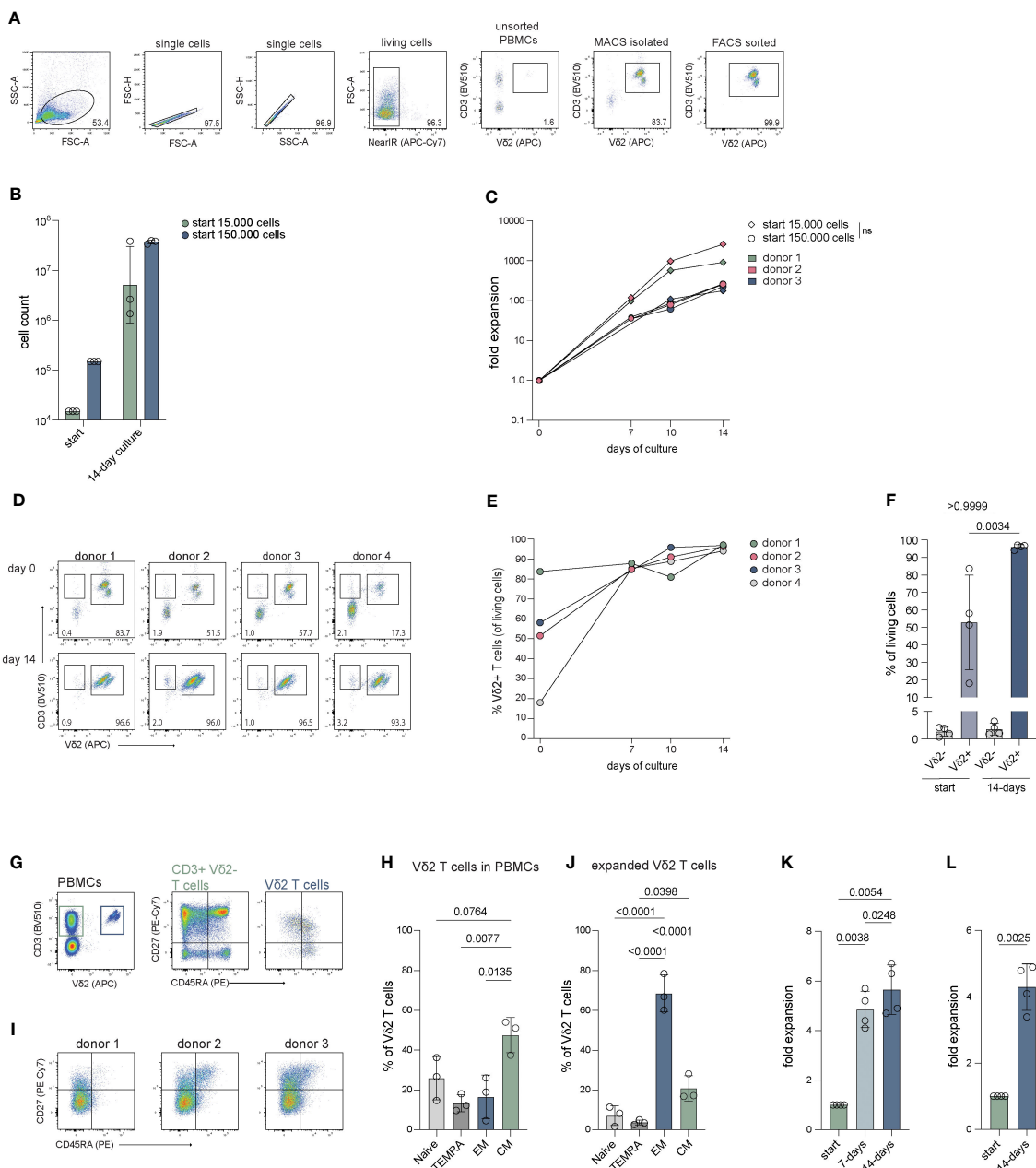


FIGURE 1

Cell count and fold expansion of Vδ2<sup>+</sup> T cells after 14 days of expansion. The cells were isolated through mouse anti-human Vδ2 TCR and anti-mouse IgG bead MACS enrichment, with or without additional FACS sort, and expanded straight after isolation or previously expanded Vδ2<sup>+</sup> T cells were submitted to a new round of expansion. Expanded cells were stained for CD27 and CD45RA to determine their differentiation status. **(A)** Representative flow cytometry plots and gating strategy showing the percentage of Vδ2<sup>+</sup> T cells in unsorted PBMCs, after Vδ2 TCR specific MACS isolation and after an additional FACS sort for Vδ2<sup>+</sup> T cells. **(B)** The number of Vδ2<sup>+</sup> T cells used at the start of expansion, 15,000 and 150,000, and the number of cells yielded after the 14-day expansion (n=3). **(C)** The fold expansion of the Vδ2<sup>+</sup> T cells for each donor of day 7, 10 and 14 relative to the start numbers, 15,000 and 150,000, respectively (n=3). **(D)** Flow cytometry plots showing the percentage of the Vδ2<sup>+</sup> cells after isolation (top row) using only the anti-Vδ2 TCR antibody combined with anti-mouse IgG beads and MACS separation, without FACS sort, and after a 14-day expansion period (bottom row) for four donors. **(E)** The percentage of Vδ2<sup>+</sup> T cells after 7, 10 and 14 days of expansion and **(F)** the percentage of CD3<sup>+</sup>Vδ2<sup>-</sup> T cells and CD3<sup>+</sup>Vδ2<sup>+</sup> T cells before and after 14 days of expansion. **(G)** Representative flow cytometry plots showing the frequency of CD3<sup>+</sup>Vδ2<sup>-</sup> and CD3<sup>+</sup>Vδ2<sup>+</sup> T cells in PBMCs (left plot) and the frequency of naive (T<sub>naive</sub>, CD27<sup>+</sup>CD45RA<sup>+</sup>), terminally differentiated Effector Memory RA (T<sub>EMRA</sub>, CD27<sup>-</sup>CD45RA<sup>+</sup>), Effector Memory (T<sub>EM</sub>, CD27<sup>-</sup>CD45RA<sup>-</sup>) and Central Memory (T<sub>CM</sub>, CD27<sup>+</sup>CD45<sup>-</sup>) T cells for the CD3<sup>+</sup>Vδ2<sup>-</sup> (middle plot) and CD3<sup>+</sup>Vδ2<sup>+</sup> T cells (right plot) in PBMCs before isolation. **(H)** Summary of the percentage of T<sub>naive</sub>, T<sub>EMRA</sub>, T<sub>EM</sub> and T<sub>CM</sub> subsets in CD3<sup>+</sup>Vδ2<sup>+</sup> T cells before isolation, as determined in **(H, I)** Flow cytometry plots of three donors showing the distribution of the T<sub>naive</sub>, T<sub>EMRA</sub>, T<sub>EM</sub> and T<sub>CM</sub> subsets in the total Vδ2<sup>+</sup> T cell population after a 14-day expansion culture. Gating is based on freshly isolated CD3<sup>+</sup> cells in total PBMCs from a reference donor. **(J)** Summary of the data in **(I, K)** The fold expansion of Vδ2<sup>+</sup> T cells that were expanded for 14 days that were, straight from culture, submitted to a new expansion culture of 14-days (n=4). **(L)** Fold expansion of Vδ2<sup>+</sup> T cells that were previously expanded for 14 days after which they were cryopreserved for at least four weeks, thawed and submitted to a new expansion culture of 14 days (n=4). The data is shown as the mean and standard deviation of the donors and data from each donor represents the mean of triplicates. Data was analyzed by a one-way ANOVA followed by Tukey's multiple comparisons test **(B, C, F, H, J, K)** or a student's T-test **(L)**.

## FACS-sorted V $\delta$ 2 cells expand equally to non FACS-sorted cells

To assess if the process of FACS sorting following MACS enrichment affects the expansion potential of the isolated  $\gamma\delta$  T cells, the expansion capacities of isolated V $\delta$ 2<sup>+</sup> T cells with or without FACS sort were compared from the same donors. The expansion of cells that were isolated using only MACS enrichment generated 12-43 million cells (Supplementary Figure 1C, adjusted to percentage V $\delta$ 2<sup>+</sup> cells,  $n=4$ ) and displayed a similar fold expansion compared to cells from the same donor that were isolated through both MACS and FACS sort (Supplementary Figure 1D,  $n=3$ ). Thus, FACS sorting does not compromise the expansion capacity of V $\delta$ 2<sup>+</sup> T cells.

## The expansion of V $\delta$ 2 T cells is not compromised by outgrowth by other cell types

Given the generic character of the feeder-based expansion protocol, other T cell subsets may potentially overgrow the  $\gamma\delta$  T cells during the expansion phase. To investigate whether the purity of the V $\delta$ 2<sup>+</sup> T cells could be compromised by the contamination of  $\alpha\beta$  T cells or other cell types, less pure V $\delta$ 2<sup>+</sup> T cells isolated using direct targeting MACS isolation ( $n=4$ ) or pan  $\gamma\delta$  T cells isolated using untouched MACS isolation ( $n=2$ ) without FACS sort were expanded and significant co-expansion of other cells was monitored.

After direct V $\delta$ 2<sup>+</sup> targeting MACS isolation, the percentage of CD3<sup>+</sup>V $\delta$ 2<sup>+</sup> T cells ranged between 17-84% (Figure 1D top panel, E, F) and between 0.4-2% of the isolated cells was CD3<sup>+</sup>V $\delta$ 2<sup>-</sup>. Most V $\delta$ 2 negative cells that remain after MACS isolation were not T cells (CD3<sup>-</sup>). The percentage of CD3<sup>+</sup>V $\delta$ 2<sup>+</sup> T cells significantly increased to 93-97% after a 14-day expansion period (Figure 1E). The CD3<sup>+</sup>V $\delta$ 2<sup>-</sup> cell population expanded alongside the CD3<sup>+</sup>V $\delta$ 2<sup>+</sup> T cells during the 14-day culture though their relative presence did not significantly increase (Figures 1D, F). The CD3<sup>-</sup> cells were no longer present after the expansion (Figure 1D, bottom panel).

From two donors,  $\gamma\delta$  T cells were isolated from PBMCs using the TCR $\gamma/\delta$ + T Cell Isolation Kit (Miltenyi), which comprised of 49% and 80% V $\delta$ 2<sup>+</sup> T cells. Expansion of these  $\gamma\delta$  T cells yielded 20-27 million cells of which 76-96% were V $\delta$ 2<sup>+</sup> T cells and 3-20% are CD3<sup>+</sup>V $\delta$ 2<sup>-</sup> cells (Supplementary Figures 1E-G).

Altogether, this indicates that - during the feeder-based expansion protocol - the purity of V $\delta$ 2<sup>+</sup> T cells is not compromised by overgrowth by other cells, such as  $\alpha\beta$  T cells.

## The V $\delta$ 2 T cells show an effector phenotype after expansion

To assess the phenotype and functionality of the expanded V $\delta$ 2<sup>+</sup> T cells, the cells were immunophenotyped before and after expansion using surface expression of CD27 and CD45RA.

Before expansion, 38-54% of the V $\delta$ 2<sup>+</sup> T cells were primarily of a central memory (T<sub>CM</sub>; CD27<sup>+</sup>CD45RA<sup>-</sup>) phenotype followed by a naïve phenotype (T<sub>naive</sub>; CD27<sup>+</sup>CD45RA<sup>+</sup>), with 15-36% an effector memory phenotype (T<sub>EM</sub>; CD27<sup>-</sup>CD45RA<sup>-</sup>) with 5-26% (Figures 1G, H). The percentage of terminally differentiated effector memory RA (T<sub>EMRA</sub>; CD27<sup>-</sup>CD45RA<sup>+</sup>) cells was 9-18%. After expansion, most V $\delta$ 2<sup>+</sup> T cells exhibited a T<sub>EM</sub> phenotype which comprised 60-79% of the cells, followed by a T<sub>CM</sub> phenotype containing 17-28% of the cells (Figures 1I, J). The T<sub>naive</sub> and the T<sub>EMRA</sub> subsets contained the fewest cells with 2-11% and 3-5%, respectively.

## Previously expanded V $\delta$ 2 T cells can be expanded further using this PHA based TCR triggering culture method

To examine if V $\delta$ 2<sup>+</sup> T cells can be expanded further after initial expansion, V $\delta$ 2<sup>+</sup> T cells were submitted to a new 14-day expansion culture straight from the first 14-day expansion. The V $\delta$ 2<sup>+</sup> T cells ( $n=4$ ) reached a 4.1-5.7-fold expansion after the first seven days and a 4.7 to 6.7-fold expansion after the second full 14-day expansion period (Figure 1K).

To investigate whether 14-day expanded V $\delta$ 2<sup>+</sup> T cells can be expanded further after cryopreservation, frozen 14-day expanded V $\delta$ 2<sup>+</sup> T cells were thawed and submitted to a new 14-day expansion. Frozen, previously expanded V $\delta$ 2<sup>+</sup> T cells ( $n=4$ ) showed a 4.3 to 4.9-fold expansion after 14 days (Figure 1L).

Although reduced compared to the first expansion, previously expanded V $\delta$ 2<sup>+</sup> T cells can be expanded further using the expansion protocol described in this report.

## Direct targeted MACS isolation combined with FACS sort and this expansion protocol can be used to expand both V $\delta$ 1 and V $\delta$ 2 subsets

To investigate if the direct isolation protocol can be used to purify and isolate V $\delta$ 1<sup>+</sup> T cells and if their expansion would be equal to that of V $\delta$ 2<sup>+</sup> T cells, both V $\delta$ 1<sup>+</sup> and V $\delta$ 2<sup>+</sup> T cells were isolated from the same PBMC donors and to compare their expansion competence ( $n=3$ ).

Direct positive isolation of V $\delta$ 1<sup>+</sup> and V $\delta$ 2<sup>+</sup> T cells by magnetic beads (MACS) yielded approx. 90% V $\delta$ 1<sup>+</sup> or V $\delta$ 2<sup>+</sup> pure populations, with purity being increased to > 99% purity by additional FACS sort (Supplementary Figure 1H). Over the culture period of 14 days, the two subsets expanded within a similar range through the first week (day 7) with an expansion of 29-fold for V $\delta$ 1<sup>+</sup> and 19-fold for V $\delta$ 2<sup>+</sup> T cells on average (Supplementary Figure 1I). At day 14, expansion of both subsets was high, with expansion of the V $\delta$ 2<sup>+</sup> subset exceeding that of the V $\delta$ 1<sup>+</sup> subset with an average of 1248-fold over a 380-fold for V $\delta$ 1<sup>+</sup> T cells (Supplementary Figure 1I).

This isolation and expansion method can thus be applied to both  $V\delta 1^+$  and  $V\delta 2^+$  T cells to yield high cell numbers for downstream use.

## Specific isolation combined with PHA activation generates more pure cell populations compared to specific stimulation methods

Activation and expansion through specific stimulation of  $\gamma\delta$  T cells in total PBMCs by  $\gamma\delta$  TCR targeting, using immobilized antibodies is often used in the field to obtain  $V\delta 1^+$  T cells,  $V\delta 2^+$  T cells or a mixture of  $\gamma\delta$  T cell populations (70–72). To determine how the efficacy of our specific isolation and expansion protocols of  $\gamma\delta$  T cells (MACS+FACS) and PHA activation is similar to these strategies, the purity and fold expansion of  $V\delta 1$  and  $V\delta 2$  T cells obtained through both methods were analyzed. PBMCs were either subjected to anti-PAN $\gamma\delta$  TCR, anti- $V\delta 1$  TCR or anti- $V\delta 2$  TCR mediated MACS isolation, followed by FACS sort, or PBMCs were plated on antibody coated plates directly. Sorted cells were stimulated with PHA, feeder cells and cytokines. PBMCs were supported with cytokines at the beginning of the 14-day expansion period ( $n=4$ ).

Prior to isolation or expansion from PBMCs,  $V\delta 1^+$  and  $V\delta 2^+$  T cells constituted only a small fraction of  $CD3^+$  T cell population (Figure 2A). Expansion of the MACS+FACS sorted cells generated >99% pure  $CD3^+$  T cells (Figure 2B). In contrast, plate bound activation of PBMCs yielded between 75–96%  $CD3^+$  cells, which still consisted of a significant number of conventional  $\alpha\beta$  T cells (Supplementary Figures 2A–C). To enrich this population for  $\gamma\delta$  T cells, usually  $\alpha\beta$  T cells are depleted, which in these experiments reduced the  $CD3^+$  population to 27–90% after  $\alpha\beta$  T cell depletion (Figure 2B; Supplementary Figures 2A–C). Expanded cells after initial PAN $\gamma\delta$  sort consisted primarily of  $V\delta 2^+$  T cells, while specific PAN $\gamma\delta$  antibody based expansion followed by an  $\alpha\beta$  T depletion generated a variable mix of  $V\delta 1^+$  T cells and  $V\delta 2^+$  T cells, contaminated with a fraction of  $V\delta 1^+/V\delta 2^-$  T cells (Figures 2B, C). The cells sorted directly with the  $V\delta 1$  targeting antibody yielded >99%  $V\delta 1^+$  cells (Figures 2B, D). In comparison, plate bound activation with this antibody resulted in a cell population with only 28–62%  $V\delta 1^+$  cells (Figures 2B, D). Lastly, cells sorted using anti- $V\delta 2$  antibodies established >99%  $V\delta 2^+$  T cells (Figures 2B, E) for all donors compared to 23–96%  $V\delta 2^+$  T cells using anti- $V\delta 2$  plate bound activation (Figures 2B, E).

After expansion, cells were counted to assess differences in expansion effectivity of the different methods. One million of anti- $V\delta 1$  sorted and PHA expanded cells generated 482 million  $V\delta 1^+$  T cells on average for the four donors used and one million of cells sorted using the  $V\delta 2$  targeting antibody resulted in 588 million  $V\delta 2^+$  T cells on average (Figures 2F, G).

The methods using antibody mediated activation and outgrowth of one million PBMCs resulted on average in 7 million  $V\delta 1^+$  T cells (227-fold expansion) and 12 million  $V\delta 2^+$  T cells (159-fold expansion) using anti-PAN $\gamma\delta$  stimulation (Figures 2F, G). Anti- $V\delta 1$  stimulation of one million PBMCs yielded 5 million

$V\delta 1^+$  cells (144-fold expansion) and anti- $V\delta 2$  stimulation generated 5 million  $V\delta 2^+$  T cells (96-fold expansion) (Figures 2F, G). There was no significant difference between the cell numbers or fold expansion between directly isolated (MACS+FACS sorted) and PHA stimulated cells versus cells generated through plate bound activation by antibodies combined with  $\alpha\beta$  T cell depletion after the 14-day expansion.

## The $V\delta 1$ and $V\delta 2$ T cells show an effector phenotype after expansion

To assess effector potential, expanded  $V\delta 1^+$  and  $V\delta 2^+$  T cells were stimulated with PMA/Ionomycin for 1.5 hours and production of cytokines TNF $\alpha$  and IFN $\gamma$ , as well as granzyme B release were determined. At least 80% of  $\gamma\delta$  T cells produced TNF- $\alpha$  (Figures 3A–C). Surprisingly, only 14–60% of the  $V\delta 1^+$  T cells produced IFN- $\gamma$ , while the majority of the  $V\delta 2^+$  T cells were IFN- $\gamma$  positive (82–90%) (Figures 3A, D, E). Production of granzyme B was present in most cells before stimulation (>95%) and cells remained positive upon activation, but showed a significant decrease in MFI for granzyme B staining, possibly indicating early degranulation (Figures 3F–H).

These data show that positively isolated  $V\delta 1^+$  and  $V\delta 2^+$  T cells expanded with feeder cells, PHA, IL-2, IL-7 and IL-15 have the capacity to produce IFN- $\gamma$ , TNF- $\alpha$  and granzyme B.

## The $\gamma\delta$ T cells expanded with feeder cells, PHA, IL-2, IL-7 and IL-15 effectively kill target cells

The capacity to induce anti-tumor cytotoxicity by positively isolated and expanded  $V\delta 1^+$  and  $V\delta 2^+$  T cells from four donors was assessed in co-cultures with cell lines derived from different tumor types; WiDr cell line (colon adenocarcinoma), WM9 cell line (melanoma), HT29 cell line (colon carcinoma) and the HAP1 cell line (chronic myelogenous leukemia) which, due to its near-haploidy, is a highly useful cell line for genetic manipulation/gene knock-out approaches in future studies on mechanistic pathways (73).

The  $V\delta 1^+$  T cells derived from all donors showed effective killing of 52–65% WiDr cells, 37–57% WM9 cells, 54–75% of HT29 cells and 31–62% of HAP1 cells (background subtracted) (Figures 3I–M).  $V\delta 2^+$  T cells killed significantly fewer of each of these target cells (Figures 3I–M). Thus  $\gamma\delta$  T cells expanded using specific isolation followed by aspecific expansion effectively killed target cells from different origins with superiority of  $V\delta 1^+$  T cells over  $V\delta 2^+$  T cells.

## Pre-treatment of target cells with PAM improves HAP1 cell killing by $V\delta 2$ T cells, but not of WiDr or WM9

Due to dysregulation of the mevalonate pathway, phosphoantigen levels can accumulate in tumor cells resulting in elevated,  $V\delta 2$  TCR activating BTN3A1/3A2 complexes on the cell surface. Pre-treatment

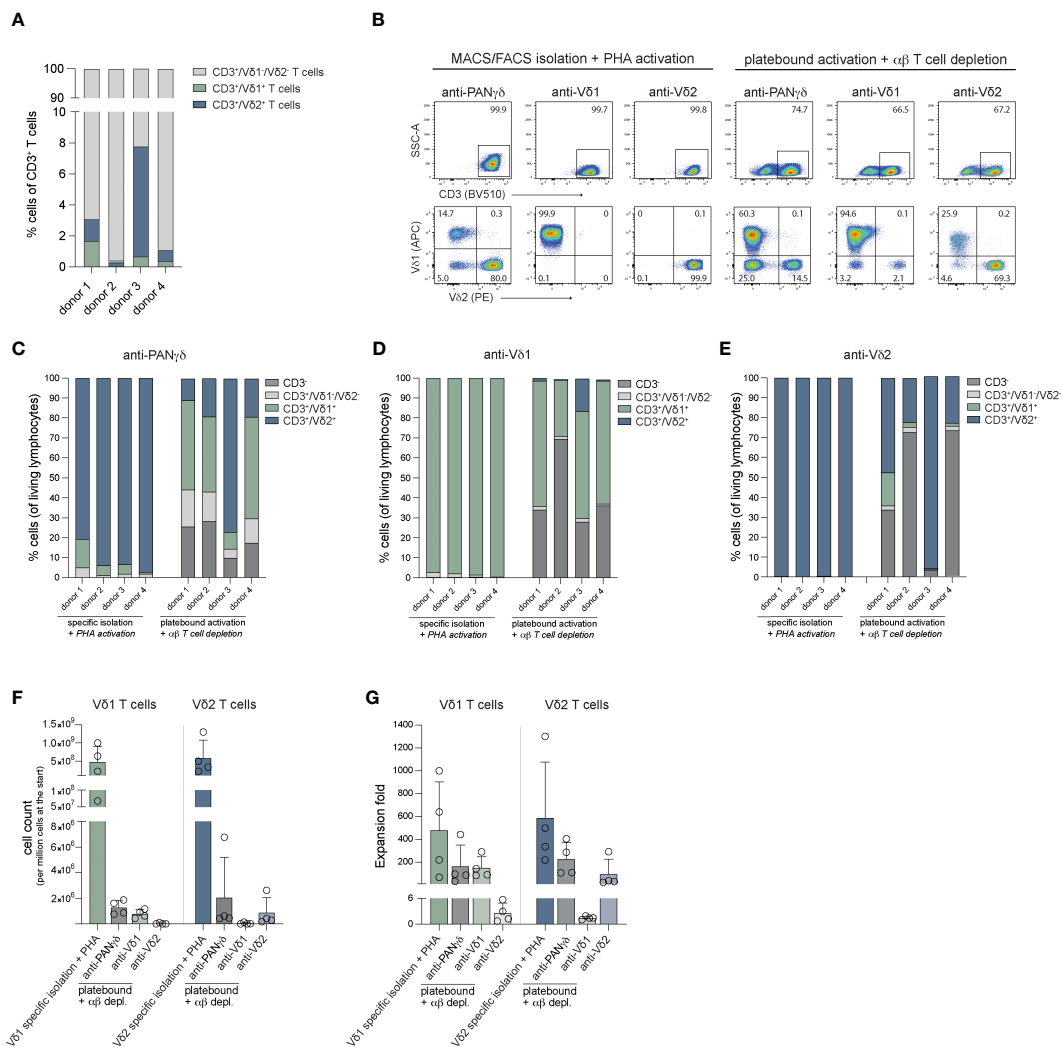


FIGURE 2

Purity and fold expansion of Vδ1<sup>+</sup> and Vδ2<sup>+</sup> cells isolated through MACS/FACS sort using anti-PANγδ/Vδ1/Vδ2 TCR antibodies and activated with PHA or expanded from PBMCs using immobilized anti-PANγδ/Vδ1/Vδ2 TCR antibodies depleted for αβ T cells after expansion. (A) The percentage of Vδ1<sup>+</sup> T cells, Vδ2<sup>+</sup> T cells and Vδ1<sup>+</sup>/Vδ2<sup>+</sup> T cells of CD3<sup>+</sup> cells in PBMCs per donor. (B) Representative flow cytometry plots of the percentage of CD3<sup>+</sup> cells (top panel) and Vδ1<sup>+</sup>/Vδ2<sup>+</sup> T cells (CD3<sup>+</sup> gated, bottom panel) after 14-days expansion of MACS/FACS isolated + PHA activated cells or cells activated using immobilized (plate bound) antibodies depleted for αβ T cells. (C) The distribution of CD3<sup>+</sup>, CD3<sup>+</sup>/Vδ1<sup>+</sup>/Vδ2<sup>+</sup>, Vδ1<sup>+</sup> and Vδ2<sup>+</sup> cells after 14-days expansion of MACS/FACS using an anti-PANγδ TCR antibody + PHA activated cells or cells activated using immobilized (plate bound) anti-PANγδ TCR antibody depleted for αβ T cells. (D) The distribution of CD3<sup>+</sup>, CD3<sup>+</sup>/Vδ1<sup>+</sup>/Vδ2<sup>+</sup>, Vδ1<sup>+</sup> and Vδ2<sup>+</sup> cells after 14-days expansion of MACS/FACS using an anti-Vδ1 TCR antibody + PHA activated cells or cells activated using immobilized (plate bound) anti-Vδ1 TCR antibody depleted for αβ T cells. (E) The distribution of CD3<sup>+</sup>, CD3<sup>+</sup>/Vδ1<sup>+</sup>/Vδ2<sup>+</sup>, Vδ1<sup>+</sup> T cells and Vδ2<sup>+</sup> T cells after 14-days expansion of MACS/FACS using an anti-Vδ2 TCR antibody + PHA activated cells or cells activated using immobilized (plate bound) anti-Vδ2 TCR antibody depleted for αβ T cells. (F) The cell counts generated from 14-days expanded of 1 million Vδ1<sup>+</sup> and Vδ2<sup>+</sup> T cells isolated through MACS/FACS sort and activated with PHA + feeder cells, or generated from 1 million PBMCs activated using immobilized (plate bound) antibodies. (G) Fold expansion of Vδ1<sup>+</sup> and Vδ2<sup>+</sup> T cells isolated through MACS/FACS sort and activated with PHA + feeder cells, or from 1 million PBMCs activated using immobilized (plate bound) antibodies.

of cell lines with the aminobiphosphonate pamidronate (PAM) can mimic this increase in phosphoantigen levels and, subsequently, potentially enhance BTN3A1/A2 mediated Vδ2<sup>+</sup> T cell activation. To test whether including PAM increases activation of the Vδ2<sup>+</sup> T cells, WiDr, WM9 and HAP1 cells were pretreated with PAM overnight before being subjected to an activation and killing assay.

Vδ2<sup>+</sup> T cells from three different donors effectively killed 35-40% WiDr cells, 15-20% WM9 cells and 25-34% HAP1 cells (background subtracted) (Figures 4A-D). Pretreatment with PAM significantly improved HAP1 cell killing by Vδ2<sup>+</sup> T cells but not of WiDr and

WM9 cells (Figure 4D). The activation state of expanded Vδ2<sup>+</sup> T cells via CD25, CD69 and CD137 was also assessed in cocultures with WiDr, WM9 and HAP1 tumor cells (Figures 4E-H). Surface expression of CD25 and CD69 was significantly increased on Vδ2<sup>+</sup> T cells cultured with WiDr cells, indicating that these target cells most strongly activated the Vδ2<sup>+</sup> T cells (Figures 4E-G). To investigate this further, the cell surface levels of butyrophilin of these cell lines were assessed through flow cytometry using an anti-BTN2A1/3A1 antibody. WiDr cells showed a higher cell surface staining compared to WM9 and HAP1 cells, which implies a potential role

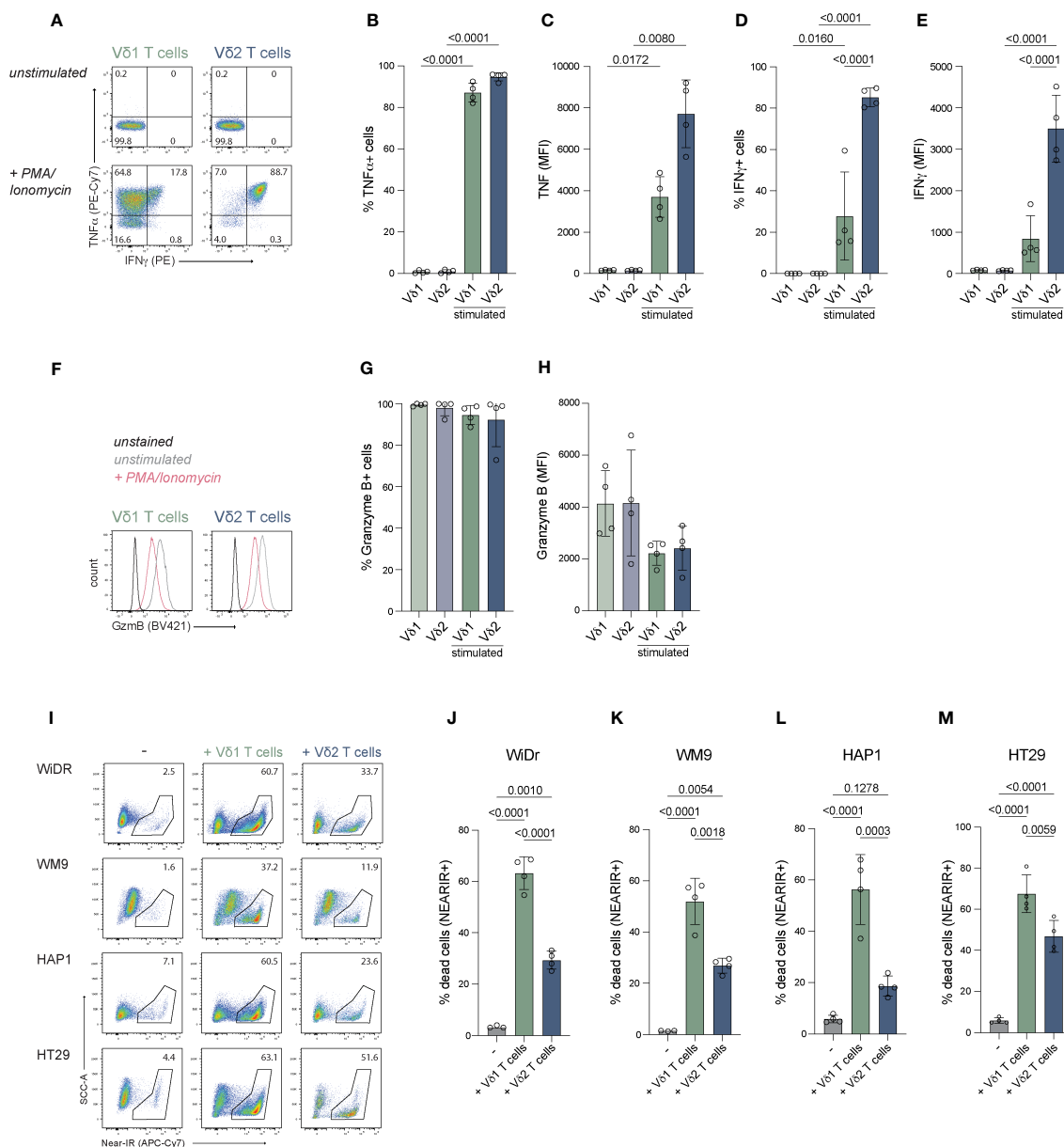


**FIGURE 3** Effector molecule production and anti-tumor function of expanded Vδ1<sup>+</sup> and Vδ2<sup>+</sup> T cells. Expanded cells were stimulated with PMA/Ionomycin to assess their potential to produce effector molecules IFN-γ, TNF-α and granzyme (B) Tumor killing capacity was assessed with a coculture of freshly expanded γδ T cells with target cells lines WiDr, WM9, HAP1 and HT29. (A) Representative flow cytometry plots showing production of IFN-γ and TNF-α by Vδ1<sup>+</sup> and Vδ2<sup>+</sup> T cells stimulated with PMA/Ionomycin for 1.5 hour or unstimulated. (B–E) Summary of the production of IFN-γ and TNF-α by Vδ1<sup>+</sup> and Vδ2<sup>+</sup> T cells stimulated with PMA/Ionomycin for 1.5 hour or unstimulated. The percentage and MFI of the cytokine positive cells is depicted (F) Representative flow cytometry plots showing the production of granzyme B by Vδ1<sup>+</sup> and Vδ2<sup>+</sup> T cells stimulated with PMA/Ionomycin for 1.5 hour or unstimulated. (G, H) Summary of the production of granzyme B by Vδ1<sup>+</sup> and Vδ2<sup>+</sup> T cells stimulated with PMA/Ionomycin for 1.5 hour or unstimulated. The percentage and MFI of the granzyme B positive cells is depicted. (I) Representative flow cytometry plots showing the frequency of dead (NEAR-IR+) WiDr, WM9, HAP1 and HT29 target cells (left column) and target cells cocultured with Vδ1<sup>+</sup> (middle column) or Vδ2<sup>+</sup> (right column) T cells. (J–M) Summary of the percentage of dead target cells, WiDr, WM9, HAP1 and HT29, only (-) or with Vδ1<sup>+</sup> or Vδ2<sup>+</sup> T cells. Data are shown as the mean and standard deviation of four donors and the data of each donor represents the mean of triplicates. Data were analyzed by a one-way ANOVA followed by Tukey's multiple comparisons test.

for butyrophilins in the higher activation of Vδ2 T cells in coculture with WiDr target cells (Supplementary Figure 3).

Altogether, these data showed that WiDr cells advance CD25 and CD69 expression on Vδ2<sup>+</sup> T cells while WM9 and HAP1 cells do not. Pre-stimulation with PAM does not alter expression of activation markers, however, does improve killing of HAP1 cells but not of WiDr or WM9 cells.

### Expansion of Vδ1 and Vδ2 T cells can be achieved from low starting numbers

γδ T cells are of great interest as a means of cellular therapy to treat cancer and understanding the functionality of these cells within tumors is important for the development and optimization of future therapies. However, the absolute amount of γδ T cells

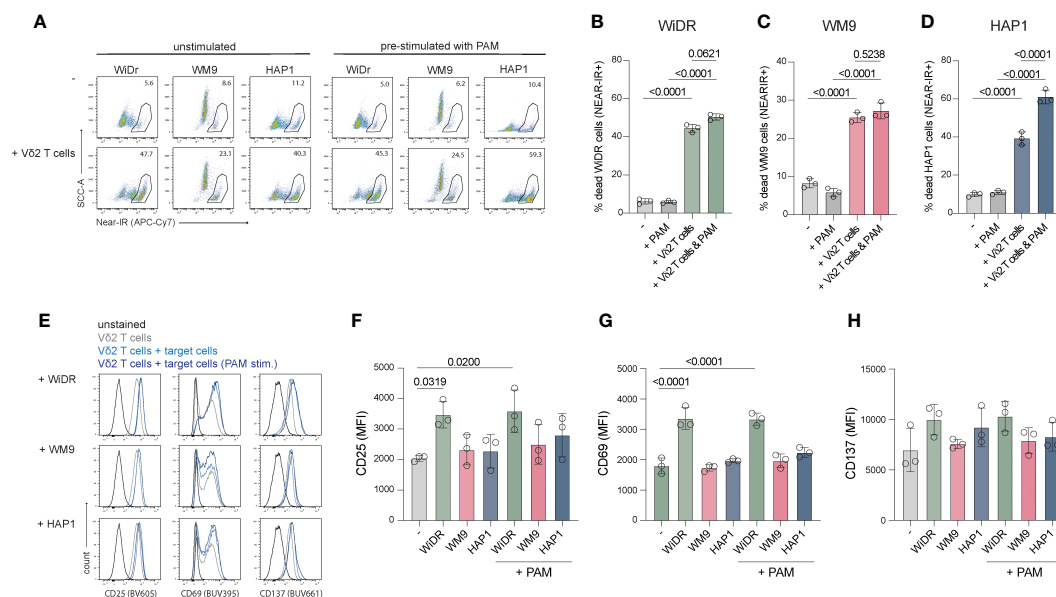


FIGURE 4

Coculture of freshly expanded  $V\delta 2^+$  T cells with target cell lines WiDr, WM9 and HAP1. 15,000 cells were plated one day prior to the coculture with or without PAM pretreatment. An effector:target ratio of 5:1 was used in a 5-hour coculture. (A) Representative flow cytometry plots showing the frequency of dead (Near-IR+) target cells only (top row) and target cells cocultured with  $V\delta 2^+$  T cells (bottom row), with or without pretreatment with PAM. (B–D) Summary of the percentage of dead target cells, WiDr, WM9 and HAP1, only (-) or with PAM treatment and/or addition of  $V\delta 2^+$  T cells. (E) Representative histograms plots showing the cell surface expression of CD25, CD69 and CD137 of  $V\delta 2^+$  T cells only or cultured with indicated target cell lines either prestimulated with PAM or not. (F–H) Overview of the MFI of CD25, CD69 and CD137 of  $V\delta 2^+$  T cells only (-) or cultured with indicated target cell lines either prestimulated with PAM or not. Gates were set using unstained  $V\delta 2^+$  T cells. Data are shown as the mean and standard deviation of the donors ( $n=3$ ). Data of each donor represents the mean of triplicates. Data were analyzed by a one-way ANOVA followed by Tukey's multiple comparisons test.

isolated from TILs in primary tumors is often very low which complicates further research. Therefore, the applicability of this expansion protocol was evaluated to expand  $V\delta 1^+$  and  $V\delta 2^+$  T cells from very low starting numbers.

Expansion of directly isolated  $V\delta 1^+$  and  $V\delta 2^+$  T cells (purity >95%) from three donors with an initial seeding density of 150 cells per well showed expansion ratios of >1000 fold at day 17 of expansion (Figure 5). After a 24-day culture period, the cells had reached a plateau in expansion. There was no significant difference observed between the  $V\delta 1^+$  and  $V\delta 2^+$  T cells.

Thus, this isolation and expansion method is also effective with low amounts of starting material and might potentially be successful in expanding tumor tissue-derived  $\gamma\delta$  T cells.

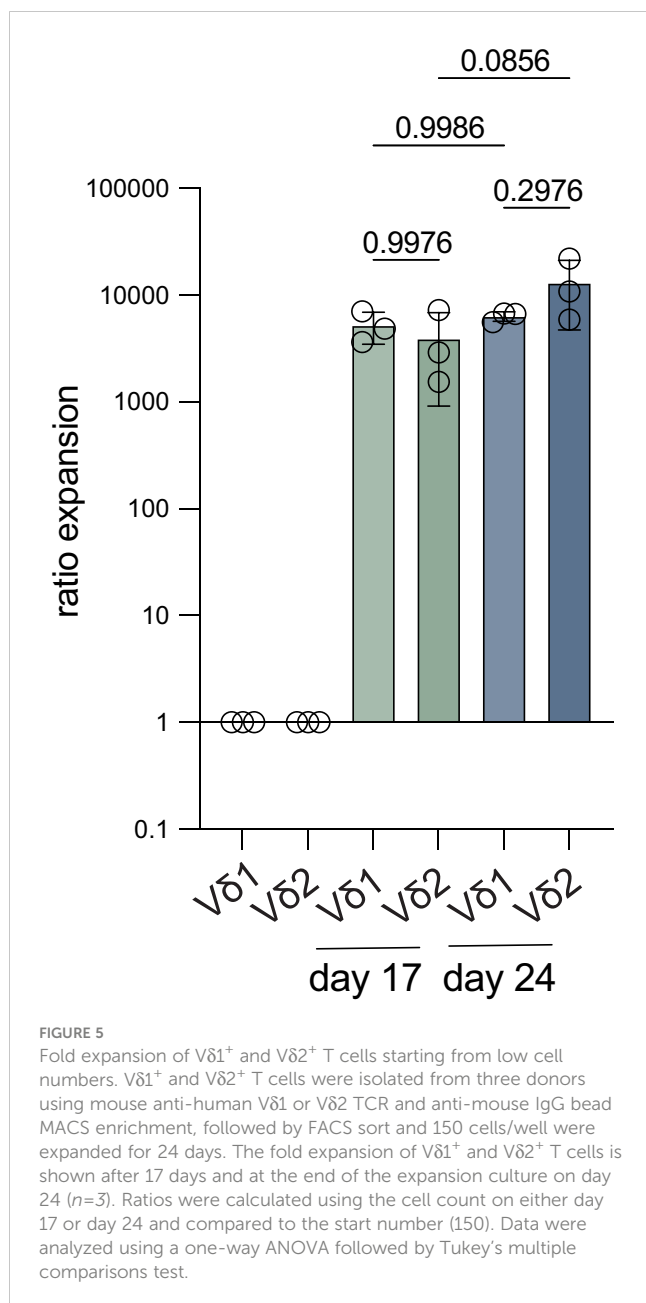
## Discussion

We described a methodology to directly isolate  $\gamma\delta$  T cells from PBMCs using MACS enrichment followed by FACS-based sorting, generating >99% pure  $\gamma\delta$  T cells. These cells effectively expand and produce effector molecules IFN- $\gamma$ , TNF- $\alpha$  and granzyme B upon stimulation. In addition, the expanded  $\gamma\delta$  T cells successfully kill cell lines of different tumor types. More importantly, we show that this method can be applied to expand  $\gamma\delta$  T cells from low cell numbers (i.e., 150 cells) and may therefore provide a tool to study  $\gamma\delta$  T cells *ex vivo*.

The here described expansion protocol is based on directly isolating  $\gamma\delta$  T cells from freshly isolated PBMCs in contrast to

most reported expansion protocols which generally deplete  $\alpha\beta$  T cells and/or CD56 positive cells (64, 68, 74–77). A disadvantage of those methods is that also a fraction of  $\gamma\delta$  T cells can be removed during this depletion step since they can express CD4, CD8 and CD56 (9, 78–82). On the other hand, the efficiency of depleting other immune cell subsets is often not reported and, in contrast to FACS sort, this depletion is not fully sufficient to remove non- $\gamma\delta$  T cells (64). As a consequence,  $\alpha\beta$  T cells, NK cells and others such as B cells and monocytes might contaminate the  $\gamma\delta$  T cell cultures (68), which is not preferable because their contribution can result in misrepresentation of the functionality of  $\gamma\delta$  T cell in *in vitro* assays.

Many established protocols use plate bound antibody activation of  $\gamma\delta$  T cells as a means of specific expansion (71, 72). Therefore, this optimized protocol was compared with a method using PBMCs stimulated with immobilized  $\gamma\delta$  T cell specific antibodies followed by an  $\alpha\beta$  depletion step post-expansion. Pre-expansion isolation and PHA stimulated cells performed at least as good as cells from PBMCs activated with immobilized TCR binding antibodies in terms of fold expansion, but, even after  $\alpha\beta$  depletion, the purity of the  $\gamma\delta$  T cells obtained with the plate-bound active activation method was lower than that of MACS/FACS sorted cells. The purity of plate bound activated  $\gamma\delta$  T cells is likely to be improved with an additional CD56+ cell depletion step is added, since NK cells likely persist due to stimulation by IL-15 in culture. Another possibility is selection for the required subset part-way or at the end of the expansion, for example by using the PAN $\gamma\delta$  TCR isolation kit offered by Miltenyi or TCR targeting isolation. Still, these would



involve another time and money consuming step and does not ensure pure populations. For example, we observed that directly after isolation a vast proportion of CD3<sup>+</sup> cells remains. Again, a steady >99% purity is guaranteed with  $\gamma\delta$  specific MACS/FACS sort prior to expansion in contrast to other methods showing donor dependent  $\gamma\delta$  T cell frequencies.

For this experiment a starting number of 6 million PBMCs per donor was used for the plate-bound method and higher numbers the  $\gamma\delta$  T cells could be achieved by scaling up the starting number. This would however require more working hours and more consumables compared to the pre-isolation method.

It is not completely clear whether having  $\alpha\beta$  T cells present during the expansion period itself is a benefit or a harm for the expansion of  $\gamma\delta$  T cells since these cells thrive on the cytokines included in culture. Though, the data on cells isolated through

MACS bead separation without FACS sort presented here showed that a small fraction of non-Vδ2 T cells do not overtake  $\gamma\delta$  T cells during expansion which indicates that the presence of other T cells does not result in an adverse effect on  $\gamma\delta$  T cell expansion. In addition, the data shown in this report supports that other cell types such as NK cells, B cells and monocytes most likely do not grow out using this MACS isolation and expansion method.

During cultures including other cell types, the  $\gamma\delta$  T cells may receive survival signals from these cell types that facilitate the expansion. One study suggests that  $\gamma\delta$  T cells expand better when the other T cells are in the same culture (83). The culture method proposed in this report includes feeder cells comprised of irradiated PBMCs and EBV transformed B cells which may account for these signals. Evaluation of this culture method with addition or substitution of specific (feeder) cells in future may provide more insights into benefit of the other cell types during expansion.

This study is not the first to include a FACS sort for  $\gamma\delta$  T cell isolation. The added benefit of the protocol described here lies in the combination of MACS isolation and FACS sort, which makes it a very efficient isolation method in terms of yield and consumption of time. Cho and colleagues uses positive selection of Vδ2 T cells solely through FACS sort prior to expansion using K562 feeder cells, anti-CD3/28 and IL-2 (84). Merely a FACS sort is likely to obtain a pure  $\gamma\delta$  T cell population from PBMCs, however, FACS sorting  $\gamma\delta$  T cells (0.5-5% of CD3<sup>+</sup> T cells) is very time-consuming. The pre-enrichment of  $\gamma\delta$  T cells by MACS isolation (purity  $\gamma\delta$  T cells of total cells: 80-90%) as described here, greatly reduces the time necessary to FACS sort the cells.

The expansion ratio for Vδ1 and Vδ2 T cells using the protocol described here (starting at 150,000 cells) range between 200 to 2000-fold. These cells can be expanded for a second time, either from culture or cryopreservation, allowing the generation of more cells and repeat or scale up experiments without the need of new  $\gamma\delta$  T cell isolation. A large fraction of  $\gamma\delta$  T cells die during or shortly after thawing of the cells after cryopreservation which can be problematic when these cells would immediately be used for functional assays. Restimulating the cells ensures a higher percentage of living cells after culture which can be used for functional analyses. Validation of the phenotype and functionality of the generated  $\gamma\delta$  T cells may be applied to ensure that the generated cells are still suitable for experimental use.

Ferry and colleagues depleted  $\alpha\beta$  T cells and CD56<sup>+</sup> NK cells from PBMCs and stimulated  $\gamma\delta$  T cell expansion using OKT-3 (anti-CD3) in combination with IL-15 after which they depleted Vδ2 T cells and focused on generating multi-applicable Vδ1 T cells (64). Interestingly, when they compared expansion of the Vδ1 T cells with OKT-3 + IL-15 to PHA + IL-2 or IL-7 they observed a better yield with OKT-3 compared to PHA conditions. Moreover, the OKT-3 activated Vδ1 T cells showed higher expression of activation markers CD69 and NKG2D. However, expansion factors reached with these protocols ranged between 10 to 48-fold using OKT-3 + IL-15 within 20-30 days, while we reached a >400-fold expansion for Vδ1 T cells with PHA and feeder cells in 14 days. This difference could be explained by the use of feeder cells in this protocol. Another reason could be the source of the PHA. The PHA (HA-16) used in this report has repeatedly been confirmed to have

high efficiency and the authors potentially used PHA from a different source (73, 85, 86).

We were able to expand 150 V $\delta$ 1 and V $\delta$ 2 T cells to 0.8-3.3 million cells in 3.5 weeks, corresponding to an expansion ratio between 5.600-22.000. De Vries and colleagues FACS sorted between 168 and 3775  $\gamma\delta$  T cells derived from colon cancer tissue which were expanded for 3-4 weeks using PHA, IL-2 and IL-15, reaching a 2000 to 170.000-fold expansion (87). An explanation for the higher expansion ratios achieved in that study may be a difference in activation state of the isolated cells  $\gamma\delta$  T cells from tumor tissue. Therefore, exploring the potential of this optimized protocol with  $\gamma\delta$  T cells extracted from tumor biopsies would be interesting. Another explanation is the IL-2 concentration of 1000 units/ml used while the expansion medium used here contained 120 units/ml IL-2. Whether the protocol described here can be further optimized in terms of cytokine concentrations or inclusion of other immune cell activating cytokines such as IL-4, IL-18 and IL-21, used in several other expansion protocols, needs further investigation.

Functionality of expanded  $\gamma\delta$  T cells was confirmed by lysis of WiDr, WM9, HT29 and HAP1 tumor cells. To gain more insight in the function of the cells, additional parameters including proliferation, functional persistence and exhaustion marker expression could be investigated.

Interestingly, Correia and colleagues showed higher cytotoxicity towards leukemia-derived cell lines by PHA-expanded  $\gamma\delta$  T cells over bromohydrin pyrophosphate (HMB-PP)-expanded  $\gamma\delta$  T (65). Expansion with PHA predominantly generated V $\delta$ 1  $\gamma\delta$  T cells from peripheral blood lymphocytes with higher expression of NCRs, while HMB-PP stimulation generated V $\delta$ 2 cells with low NCR expression. These data suggest that TCR triggering via crosslinking by PHA generates a population of  $\gamma\delta$  T cells with a higher killing capacity compared to phosphoantigen stimulated expansion. More importantly, the NCR expression by V $\delta$ 1 T cells may explain why these cells were superior over V $\delta$ 2 cells in the coculture assays demonstrated in this report. Validation and comparison of NCR expression by the expanded cells could provide more insights in the difference in functionality between the two types. In this context, it may be worthwhile to note that despite a similar anti- $\gamma\delta$  TCR MACS isolation method, PHA stimulation in the experiments described here show robust V $\delta$ 2 T cell expansion in PAN $\gamma\delta$  sorted cells, while the manuscript by Correia and colleagues showed that PHA stimulation preferences V $\delta$ 1 outgrowth over V $\delta$ 2 T cells, pointing to the need for more in depth research on the topic.

WiDr tumor cells have a higher cell surface expression of BTN3A1 compared to the WM9 and HAP1 cell lines, which could explain the higher killing percentage and significant increase of CD25 and CD69 on the challenged V $\delta$ 2 T cells because BTNs are well described stimulants of the V $\delta$ 2 TCR. PAM stimulation of HAP1 cells improved killing of these cells by V $\delta$ 2 T cells, while it did not for WiDr and WM9 cells. Stimulation with PAM may promote the structural change of the BTN3A1/A2 complex on HAP1 cells, accelerating V $\delta$ 2 TCR signaling, while (regulation of) the conformational change of BTN3A1/A2 on WiDr and WM9 may differ.

Most reported expansion methods only focus on V $\delta$ 2 T cells while V $\delta$ 1 T cells also have pro- and anti-tumor potential which

renders these cells highly relevant to investigate (42, 88). For example, it has been found that the V $\delta$ 1 T cells subset is most prevalent in TILs extracted from melanoma (33, 89). Importantly, these cells were reactive towards both allogeneic and autologous melanoma (89). In addition, V $\delta$ 1 T cells showed robust cytotoxicity against colorectal cancer (CRC), hepatocellular cancer (HCC) and leukemia *in vitro* (65, 71, 90). In contrary, it has been shown that IL-17 produced by V $\delta$ 1 cells recruits myeloid derived suppressor cells and that they suppress  $\alpha\beta$  T cell function and DC maturation (91, 92). Therefore, it is important to expand both subsets as is possible with the direct MACS and FACS sort isolation described in this study.

The V $\delta$ 1 or V $\delta$ 2 subsets are most studied in  $\gamma\delta$  T cells research while V $\delta$ 3 T cells are also found in the blood and in tumors (87). Whether this subtype can also be expanded to generate large quantities of cytotoxic  $\gamma\delta$  T cells using the protocol described here has to be explored. Lastly, generation of CAR  $\gamma\delta$  T cells for immunotherapy is emerging in the field. Most protocols involve retroviral transduction of the CAR construct after  $\gamma\delta$  specific activation, followed by the expansion phase (64, 71, 93, 94). Addition of a transduction to the protocol described here is most likely plausible, though compatibility and productivity would require experimental validation.

## Data availability statement

The original contributions presented in the study are included in the article/Supplementary Material. Further inquiries can be directed to the corresponding author.

## Ethics statement

The studies involving humans were approved by Sanquin Ethical Advisory Council, Sanquin, Amsterdam. The studies were conducted in accordance with the local legislation and institutional requirements. The participants provided their written informed consent to participate in this study.

## Author contributions

TV: Conceptualization, Formal analysis, Investigation, Methodology, Validation, Visualization, Writing – original draft, Writing – review & editing. AP: Writing – review & editing. TJ: Writing – review & editing. LK: Writing – review & editing. MD: Validation, Investigation, Writing – review & editing. RS: Funding acquisition, Supervision, Writing – review & editing. Sv: Supervision, Writing – review & editing.

## Funding

The author(s) declare financial support was received for the research, authorship, and/or publication of this article. This work was supported by grants from the Dutch Research Council (Grant

NWO-VIDI 91719369 to RS) and the Landsteiner Foundation for Blood Transfusion Research (LSBR Fellowship 1842F to RS).

## Conflict of interest

The authors declare that the research was conducted in the absence of any commercial or financial relationships that could be construed as a potential conflict of interest.

## Publisher's note

All claims expressed in this article are solely those of the authors and do not necessarily represent those of their affiliated organizations, or those of the publisher, the editors and the reviewers. Any product that may be evaluated in this article, or claim that may be made by its manufacturer, is not guaranteed or endorsed by the publisher.

## Supplementary material

The Supplementary Material for this article can be found online at: <https://www.frontiersin.org/articles/10.3389/fimmu.2024.1336870/full#supplementary-material>

### SUPPLEMENTARY FIGURE 1

The purity of V $\delta$ 2<sup>+</sup> T cells isolated with mouse anti-human V $\delta$ 2 TCR and anti-mouse IgG bead MACS enrichment followed by a V $\delta$ 2<sup>+</sup> FACS sort during the 14-day expansion. (A) Flow cytometry plots of three donors showing the percentage of V $\delta$ 2<sup>+</sup> T cells on day 0 (start), 7, 10 and 14. (B) Summary of the percentage of the data in (A) ( $n=3$ ). Data of the 150.000 start condition is shown.

Cells were isolated using mouse anti-human V $\delta$ 2 TCR and anti-mouse IgG bead MACS enrichment, with or without further purification using a FACS sort, or using untouched MACS isolation with the TCR $\gamma$ / $\delta$ + T Cell Isolation kit. CD3<sup>+</sup>V $\delta$ 2<sup>+</sup> and CD3<sup>+</sup>V $\delta$ 2<sup>-</sup> cells expansion were assessed. (C) Cell count of V $\delta$ 2<sup>+</sup> cells isolated using anti-V $\delta$ 2 MACS bead separation only after 7, 10 and 14 days of culture to expand the cells ( $n=4$ ). Counts are adjusted to the purity of the cells on the indicated days. (D) Comparison of the fold expansion of V $\delta$ 2<sup>+</sup> cells isolated using anti-V $\delta$ 2 MACS bead separation only or with an additional FACS purification ( $n=3$ ). The cells from the same donors are compared. Counts that are used to calculate the fold expansion are adjusted to the purity of the cells on the indicated days. (E) Flow cytometry plots illustrating the percentage of CD3<sup>+</sup>V $\delta$ 2<sup>-</sup> and CD3<sup>+</sup>V $\delta$ 2<sup>+</sup> of cells isolated with the TCR $\gamma$ / $\delta$ + T Cell Isolation Kit after 14 days expansion ( $n=2$ ). (F) Cell count of CD3<sup>+</sup>V $\delta$ 2<sup>+</sup> T cells isolated using the TCR $\gamma$ / $\delta$ + T Cell Isolation Kit before and after 14-days expansion ( $n=2$ ) (G) Percentage of CD3<sup>+</sup>V $\delta$ 2<sup>+</sup> T cells in the total population isolated using the TCR $\gamma$ / $\delta$ + T Cell Isolation Kit before and after 14-days expansion ( $n=2$ ). Comparison of the expansion competence of V $\delta$ 1<sup>+</sup> T and V $\delta$ 2<sup>+</sup> T cells of the same donors starting at 150.000 cells per well. The cells were isolated through mouse anti-human V $\delta$ 1 TCR or V $\delta$ 2 TCR and anti-mouse IgG bead MACS enrichment and further purified using FACS sort. (H) Representative flow cytometry plots of the percentage of V $\delta$ 1<sup>+</sup> T cells and V $\delta$ 2<sup>+</sup> T cells in PBMCs, after V $\delta$ 1<sup>+</sup> or V $\delta$ 2<sup>+</sup> T cells specific MACS isolation and after an additional SORT of V $\delta$ 1<sup>+</sup> or V $\delta$ 2<sup>+</sup> T cells before expansion. (I) The expansion ratio of V $\delta$ 1<sup>+</sup> compared to V $\delta$ 2<sup>+</sup> T cells after seven days and at the end of the expansion culture on day 14. Ratios were calculated using the cell count on either day 7 or day 14 and compared to the start number (150.000). Data was analyzed using a one-way ANOVA followed by Tukey's multiple comparisons test (B, I) followed by Tukey's multiple comparisons test or by using a student's T-test (D).

### SUPPLEMENTARY FIGURE 2

The purity of V $\delta$ 1 and V $\delta$ 2 T cells generated from PBMCs activated with immobilized (A) PAN $\gamma$  $\delta$  TCR, (B) V $\delta$ 1 TCR and (C) V $\delta$ 2 TCR targeting antibodies before and after  $\alpha$  $\beta$  T cell depletion.

### SUPPLEMENTARY FIGURE 3

Cell surface expression profiles of BTN3A1/2/3 by WiDr, WM9 and HAP1 cell lines. Represented is a flow cytometry plot of WiDr (green), WM9 (pink) and HAP1 (blue) cells incubated with anti-BTN3A1/2/3 and anti-IgG1 (APC). Included is a background control of anti-IgG1 only on WiDr cells (black) which is representative for the background on WM9 and HAP1 cells.

## References

- Lo Presti E, Dieli F, Meraviglia S. Tumor-infiltrating  $\gamma\delta$  T lymphocytes: Pathogenic role, clinical significance, and differential programming in the tumor microenvironment. *Front Immunol* (2014) 5:1–8. doi: 10.3389/fimmu.2014.00607
- Zhao Y, Niu C, Cui J. Gamma-delta ( $\gamma\delta$ ) T cells: friend or foe in cancer development. *J Transl Med* (2018) 16:1–13. doi: 10.1186/s12967-017-1378-2
- Saura-Esteller J, de Jong M, King LA, Ensing E, Winograd B, de Gruijl TD, et al. Gamma delta T-cell based cancer immunotherapy: past-present-future. *Front Immunol* (2022) 13:1–11. doi: 10.3389/fimmu.2022.915837
- Chan KF, Duarte JDG, Ostrouska S, Behren A.  $\gamma\delta$  T cells in the tumor microenvironment—Interactions with other immune cells. *Front Immunol* (2022) 13:1–20. doi: 10.3389/fimmu.2022.894315
- Liu Y, Zhang C. The role of human  $\gamma\delta$  T cells in anti-tumor immunity and their potential for cancer immunotherapy. *Cells* (2020) 9(5):1206. doi: 10.3390/cells9051206
- Dong R, Zhang Y, Xiao H, Zeng X. Engineering  $\gamma\delta$  T cells: recognizing and activating on their own way. *Front Immunol* (2022) 13:1–15. doi: 10.3389/fimmu.2022.889051
- Wu Y, Wu W, Wong WM, Ward E, Thrasher AJ, Goldblatt D, et al. Human  $\gamma\delta$  T cells: A lymphoid lineage cell capable of professional phagocytosis. *J Immunol* (2009) 183:5622–9. doi: 10.4049/jimmunol.0901772
- Wo J, Zhang F, Li Z, Sun C, Zhang W, Sun G. The role of gamma-delta T cells in diseases of the central nervous system. *Front Immunol* (2020) 11:1–10. doi: 10.3389/fimmu.2020.580304
- Bonneville M, O'Brien RL, Born WK.  $\gamma\delta$  T cell effector functions: a blend of innate programming and acquired plasticity. *Nat Rev Immunol* (2010) 10:467–78. doi: 10.1038/nri2781
- Bottino BYC, Tambussi G, Ferrini S, Ciccone E, Varese TP, Mingari TMC, et al. Two subsets of human T lymphocytes expressing monoclonal antibodies directed to two distinct molecular forms of the receptor. *J Exp Med* (1988) 168(2):491–505. doi: 10.1084/jem.168.2.491
- Del Porto P, D'Amato M, Fiorillo MT, Tuosto L, Piccolella E, Sorrentino R. Identification of a novel HLA-B27 subtype by restriction analysis of a cytotoxic gamma delta T cell clone. *J Immunol* (1994) 153:3093–100. doi: 10.4049/jimmunol.153.7.3093
- Ciccone E, Viale O, Pende D, Malnati M, Battista Ferrara G, Barocci S, et al. Specificity of human T lymphocytes expressing a gamma/delta T cell antigen receptor. Recognition of a polymorphic determinant of HLA class I molecules by a gamma/delta clone. *Eur J Immunol* (1989) 19:1267–71. doi: 10.1002/eji.1830190718
- Deseke M, Prinz I. Ligand recognition by the  $\gamma\delta$  TCR and discrimination between homeostasis and stress conditions. *Cell Mol Immunol* (2020) 17:914–24. doi: 10.1038/s41423-020-0503-y
- Das H, Sugita M, Brenner MB. Mechanisms of Vdelta1 gammadelta T cell activation by microbial components. *J Immunol* (2004) 172:6578–86. doi: 10.4049/jimmunol.172.11.6578
- Rigau M, Ostrouska S, Fulford TS, Johnson DN, Woods K, Ruan Z, et al. Butyrophilin 2A1 is essential for phosphoantigen reactivity by gd T cells. *Science* (2020) 367(6478). doi: 10.1126/science.aay5516
- Cano CE, Pasero C, De Gassart A, Kerneir C, Gabriac M, Fullana M, et al. BTN2A1, an immune checkpoint targeting V $\gamma$ 9V $\delta$ 2 T cell cytotoxicity against Malignant cells. *Cell Rep* (2021) 36(2). doi: 10.1016/j.celrep.2021.109359
- Sebestyen Z, Scheper W, Vyborova A, Gu S, Rychnavska Z, Schiffler M, et al. RhoB mediates phosphoantigen recognition by V $\gamma$ 9V $\delta$ 2 T cell receptor. *Cell Rep* (2016) 15:1973–85. doi: 10.1016/j.celrep.2016.04.081
- Tawfik D, Groth C, Gundlach JP, Peipp M, Kabelitz D, Becker T, et al. TRAIL-receptor 4 modulates  $\gamma\delta$  T cell-cytotoxicity toward cancer cells. *Front Immunol* (2019) 10:2044. doi: 10.3389/fimmu.2019.02044

19. Li Z, Xu Q, Peng H, Cheng R, Sun Z, Ye Z. IFN- $\gamma$  enhances HOS and U2OS cell lines susceptibility to  $\gamma\delta$  T cell-mediated killing through the Fas/Fas ligand pathway. *Int Immunopharmacol* (2011) 11:496–503. doi: 10.1016/j.intimp.2011.01.001
20. Tokuyama H, Hagi T, Mattarollo SR, Morley J, Wang Q, Fai-So H, et al. V $\gamma$ 9V $\delta$ 2 T cell cytotoxicity against tumor cells is enhanced by monoclonal antibody drugs - Rituximab and trastuzumab. *Int J Cancer* (2008) 122:2526–34. doi: 10.1002/ijc.23365
21. Couzi L, Pitard V, Sicard X, Garrigue I, Hawchar O, Merville P, et al. Antibody-dependent anti-cytomegalovirus activity of human  $\gamma\delta$  T cells expressing CD16 (Fc $\gamma$ RIIIa). *Blood* (2012) 119:1418–27. doi: 10.1182/blood-2011-06-363655
22. Choi H, Lee Y, Park SA, Lee JH, Park J, Park JH, et al. Human allogenic  $\gamma\delta$  T cells kill patient-derived glioblastoma cells expressing high levels of DNAM-1 ligands. *Oncimmunology* (2022) 11:1–10. doi: 10.1080/2162402X.2022.2138152
23. Knight A, MacKinnon S, Lowdell MW. Human Vdelta1 gamma-delta T cells exert potent specific cytotoxicity against primary multiple myeloma cells. *Cytotherapy* (2012) 14:1110–8. doi: 10.3109/14653249.2012.700766
24. Groh BYV, Porcelli S, Fabbri IM, Lanier LL, Picker LJ, Anderson T, et al. Human lymphocytes bearing T cell receptor gamma/delta are phenotypically diverse and evenly distributed throughout the lymphoid system. *J Exp Med* (1989) 169(4):1277–94. doi: 10.1084/jem.169.4.1277
25. Chabab G, Boissière-Michot F, Mollevi C, Ramos J, Lopez-Crapez E, Colombo PE, et al. Diversity of Tumor-Infiltrating  $\gamma\delta$  T-Cell Abundance in Solid Cancers. *Cells* (2020) 9(6):1537. doi: 10.3390/cells9061537
26. Maniar A, Zhang X, Lin W, Gastman BR, Pauza CD, Strome SE, et al. Human gammadelta T lymphocytes induce robust NK cell-mediated antitumor cytotoxicity through CD137 engagement. *Blood* (2010) 116:1726–33. doi: 10.1182/blood-2009-07-234211
27. Liu M, Hu Y, Yuan Y, Tian Z, Zhang C.  $\Gamma\delta$ T cells suppress liver fibrosis via strong cytotoxicity and enhanced NK cell-mediated cytotoxicity against hepatic stellate cells. *Front Immunol* (2019) 10:1–15. doi: 10.3389/fimmu.2019.00477
28. Dunne MR, Madrigal-Esteban L, Tobin LM, Doherty DG. (E)-4-hydroxy-3-methyl-but-2 enyl pyrophosphate-stimulated Vgamma9Vdelta2 T cells possess T helper type 1-promoting adjuvant activity for human monocyte-derived dendritic cells. *Cancer Immunol Immunother* (2010) 59:1109–20. doi: 10.1007/s00262-010-0839-8
29. Born WK, Huang Y, Reinhardt RL, Huang H, Sun D, O'Brien RL. Chapter One -  $\gamma\delta$  T cells and B cells. *Adv Immunol* (2017) 134:1–45. doi: 10.1016/b.sai.2017.01.002
30. Brandes M, Willmann K, Lang AB, Nam KH, Jin C, Brenner MB, et al. Flexible migration program regulates  $\gamma\delta$  T-cell involvement in humoral immunity. *Blood* (2003) 102:3693–701. doi: 10.1182/blood-2003-04-1016
31. Ismaili J, Oslislagers V, Poupot R, Fournié J-J, Goldman M. Human gamma delta T cells induce dendritic cell maturation. *Clin Immunol* (2002) 103:296–302. doi: 10.1006/clim.2002.5218
32. Cordova A, Toia F, la Mendola C, Orlando V, Meraviglia S, Rinaldi G, et al. Characterization of human  $\gamma\delta$  T lymphocytes infiltrating primary Malignant melanomas. *PLoS One* (2012) 7:1–9. doi: 10.1371/journal.pone.0049878
33. Bialasiewicz AA, Ma JX, Richard G.  $\alpha\beta$ - and  $\gamma\delta$  TCR+ lymphocyte infiltration in necrotizing choroidal melanomas. *Br J Ophthalmol* (1999) 83:1069–73. doi: 10.1136/bjo.83.9.1069
34. Foord E, Arruda LCM, Gaballa A, Klynning C, Uhlin M. Characterization of ascites- And tumor-infiltrating  $\gamma\delta$  T cells reveals distinct repertoires and a beneficial role in ovarian cancer. *Sci Transl Med* (2021) 13:1–14. doi: 10.1126/scitranslmed.abb0192
35. Knight A, Piskacek M, Jurajda M, Prochazkova J, Racil Z, Zackova D, et al. Expansions of tumor-reactive Vdelta1 gamma-delta T cells in newly diagnosed patients with chronic myeloid leukemia. *Cancer Immunol Immunother* (2023) 72:1209–24. doi: 10.1007/s00262-022-03312-3
36. Juran V, Piskacek M, Tomandlova M, Sova M, Smrcka M, Kazda T, et al. CNS-13. TUMOR INFILTRATION OF GAMMA-DELTA T CELLS IN GLIOBLASTOMA. *Neuro. Oncol* (2022) 24:vii24–4. doi: 10.1093/neuonc/noac209.094
37. Gentles AJ, Newman AM, Liu CL, Bratman SV, Feng W, Kim D, et al. The prognostic landscape of genes and infiltrating immune cells across human cancers. *Nat Med* (2015) 21:938–45. doi: 10.1038/nm.3909
38. Ma C, Zhang Q, Ye J, Wang F, Zhang Y, Wevers E, et al. Tumor-infiltrating  $\gamma\delta$  T lymphocytes predict clinical outcome in human breast cancer. *J Immunol* (2012) 189:5029–36. doi: 10.4049/jimmunol.1201892
39. Inman BA, Frigola X, Harris KJ, Kuntz SM, Lohse CM, Leibovich BC, et al. Questionable relevance of  $\gamma\delta$  T lymphocytes in renal cell carcinoma. *J Immunol* (2008) 180:3578–84. doi: 10.4049/jimmunol.180.5.3578
40. Ma L, Feng Y, Zhou Z. A close look at current  $\gamma\delta$  T-cell immunotherapy. *Front Immunol* (2023) 14:1–20. doi: 10.3389/fimmu.2023.1140623
41. Kabelitz D, Serrano R, Kouakanou L, Peters C, Kalyan S. Cancer immunotherapy with  $\gamma\delta$  T cells: many paths ahead of us. *Cell Mol Immunol* (2020) 17:925–39. doi: 10.1038/s41423-020-0504-x
42. Li Y, Li G, Zhang J, Wu X, Chen X. The dual roles of human  $\gamma\delta$  T cells: anti-tumor or tumor-promoting. *Front Immunol* (2021) 11:1–13. doi: 10.3389/fimmu.2020.619954
43. Cui J, Wang N, Zhao H, Jin H, Wang G, Niu C, et al. Combination of radiofrequency ablation and sequential cellular immunotherapy improves progression-free survival for patients with hepatocellular carcinoma. *Int J Cancer* (2014) 134:342–51. doi: 10.1002/ijc.28372
44. Aoki T, Matsushita H, Hoshikawa M, Hasegawa K, Kokudo N, Kakimi K. Adjuvant combination therapy with gemcitabine and autologous  $\gamma\delta$  T-cell transfer in patients with curatively resected pancreatic cancer. *Cytotherapy* (2017) 19:473–85. doi: 10.1016/j.jcyt.2017.01.002
45. Nicol AJ, Tokuyama H, Mattarollo SR, Hagi T, Suzuki K, Yokokawa K, et al. Clinical evaluation of autologous gamma delta T cell-based immunotherapy for metastatic solid tumours. *Br J Cancer* (2011) 105:778–86. doi: 10.1038/bjco.2011.293
46. Abe Y, Muto M, Nieda M, Nakagawa Y, Nicol A, Kaneko T, et al. Clinical and immunological evaluation of zoledronate-activated V $\gamma$ 9 $\gamma\delta$  T-cell-based immunotherapy for patients with multiple myeloma. *Exp Hematol* (2009) 37:956–68. doi: 10.1016/j.exphem.2009.04.008
47. Kobayashi H, Tanaka Y, Yagi J, Osaka Y, Nakazawa H, Uchiyama T, et al. Safety profile and anti-tumor effects of adoptive immunotherapy using gamma-delta T cells against advanced renal cell carcinoma: A pilot study. *Cancer Immunol Immunother* (2007) 56:469–76. doi: 10.1007/s00262-006-0199-6
48. Bennouna J, Bompas E, Neidhardt EM, Rolland F, Philip I, Galéa C, et al. Phase-I study of Innacell  $\gamma\delta$ <sup>TM</sup>, an autologous cell-therapy product highly enriched in  $\gamma\delta$ 2 T lymphocytes, in combination with IL-2, in patients with metastatic renal cell carcinoma. *Cancer Immunol Immunother* (2008) 57:1599–609. doi: 10.1007/s00262-008-0491-8
49. Tanaka Y, Murata-Hirai K, Iwasaki M, Matsumoto K, Hayashi K, Kumagai A, et al. Expansion of human  $\gamma\delta$  T cells for adoptive immunotherapy using a bisphosphonate prodrug. *Cancer Sci* (2018) 109:587–99. doi: 10.1111/cas.13491
50. Nakajima J, Murakawa T, Fukami T, Goto S, Kaneko T, Yoshida Y, et al. A phase I study of adoptive immunotherapy for recurrent non-small-cell lung cancer patients with autologous  $\gamma\delta$  T cells. *Eur J Cardio-thoracic Surg* (2010) 37:1191–7. doi: 10.1016/j.jejts.2009.11.051
51. Izumi T, Kondo M, Takahashi T, Fujieda N, Kondo A, Tamura N, et al. Ex vivo characterization of  $\gamma\delta$  T-cell repertoire in patients after adoptive transfer of V $\gamma$ 9V $\delta$ 2 T cells expressing the interleukin-2 receptor  $\beta$ -chain and the common  $\gamma$ -chain. *Cytotherapy* (2013) 15:481–91. doi: 10.1016/j.jcyt.2012.12.004
52. Kakimi K, Matsushita H, Masuzawa K, Karasaki T, Kobayashi Y, Nagaoka K, et al. Adoptive transfer of zoledronate-expanded autologous V 39V $\delta$  2 T-cells in patients with treatment-refractory non-small-cell lung cancer: A multicenter, open-label, single-arm, phase 2 study. *J Immunother. Cancer* (2020) 8(2). doi: 10.1136/jitc-2020-0011185
53. Wada I, Matsushita H, Noji S, Mori K, Yamashita H, Nomura S, et al. Intraperitoneal injection of *in vitro* expanded V $\gamma$ 9V $\delta$ 2 T cells together with zoledronate for the treatment of Malignant ascites due to gastric cancer. *Cancer Med* (2014) 3:362–75. doi: 10.1002/cam4.196
54. Fonseca S, Pereira V, Lau C, Teixeira MDA, Bini-Antunes M, Lima M. Human peripheral blood gamma delta T cells: report on a series of healthy caucasian portuguese adults and comprehensive review of the literature. *Cells* (2020) 9:1–40. doi: 10.3390/cells9030729
55. Rong L, Li K, Li R, Liu HM, Sun R, Liu XY. Analysis of tumor-infiltrating gamma delta T cells in rectal cancer. *World J Gastroenterol* (2016) 22:3573–80. doi: 10.3748/wjg.v22.i13.3573
56. Girard P, Charles J, Cluzel C, Degeorges E, Manches O, Plumas J, et al. The features of circulating and tumor-infiltrating  $\gamma\delta$  T cells in melanoma patients display critical perturbations with prognostic impact on clinical outcome. *Oncimmunology* (2019) 8:1–16. doi: 10.1080/2162402X.2019.1601483
57. Kondo M, Izumi T, Fujieda N, Kondo A, Morishita T, Matsushita H, et al. Expansion of human peripheral blood  $\gamma\delta$  T cells using zoledronate. *J Vis Exp* (2011) 2:6–11. doi: 10.3791/3182
58. Tan WK, Tay J, Zeng J, Zheng M, Wang S. Minireview open access expansion of gamma delta T cells-A short review on bisphosphonate and K562-based methods gamma delta T cells as the next generation of effector cells for immunotherapy. *J Immunol Sci* (2018) 2:6–12. doi: 10.29245/2578-3009/2018/3.1133
59. Cabillic F, Toutirais O, Lavoué V, de la Pintièrre CT, Daniel P, Rioux-Leclerc N, et al. Aminobisphosphonate-pretreated dendritic cells trigger successful Vgamma9Vdelta2 T cell amplification for immunotherapy in advanced cancer patients. *Cancer Immunol Immunother* (2010) 59:1611–9. doi: 10.1007/s00262-010-0887-0
60. Nussbaumer O, Gruenbacher G, Gander H, Komuczki J, Rahm A, Thurnher M. Essential requirements of zoledronate-induced cytokine and  $\gamma\delta$  T cell proliferative responses. *J Immunol* (2013) 191:1346–55. doi: 10.4049/jimmunol.1300603
61. Wang H, Sarikonda G, Puan K-J, Tanaka Y, Feng J, Giner J-L, et al. Indirect stimulation of human V $\gamma$ 2V $\delta$ 2 T cells through alterations in isoprenoid metabolism. *J Immunol* (2011) 187:5099–113. doi: 10.4049/jimmunol.1002697
62. Nada MH, Wang H, Workalemahu G, Tanaka Y, Morita CT. Enhancing adoptive cancer immunotherapy with V $\gamma$ 2V $\delta$ 2 T cells through pulse zoledronate stimulation. *J Immunother Cancer* (2017) 5:1–23. doi: 10.1186/s40425-017-0209-6
63. Bold A, Gross H, Holzmann E, Knop S, Hoeres T, Wilhelm M. An optimized cultivation method for future *in vivo* application of  $\gamma\delta$  T cells. *Front Immunol* (2023) 14:1–13. doi: 10.3389/fimmu.2023.1185564

64. Ferry GM, Agbuduwe C, Forrester M, Dunlop S, Chester K, Fisher J, et al. and robust single-step method for CAR-V $\delta$ 1  $\gamma\delta$ T cell expansion and transduction for cancer immunotherapy. *Front Immunol* (2022) 13:1–13. doi: 10.3389/fimmu.2022.863155
65. Correia DV, Fogli M, Hudspeth K, Gomes Da Silva M, Mavilio D, Silva-Santos B. Differentiation of human peripheral blood V $\delta$ 1+ T cells expressing the natural cytotoxicity receptor NKp30 for recognition of lymphoid leukemia cells. *Blood* (2011) 118:992–1001. doi: 10.1182/blood-2011-02-339135
66. Almeida AR, Correia DV, Fernandes-Platzgummer A, Da Silva CL, Da Silva MG, Anjos DR, et al. Delta one T cells for immunotherapy of chronic lymphocytic leukemia: Clinical-grade expansion/differentiation and preclinical proof of concept. *Clin Cancer Res* (2016) 22:5795–804. doi: 10.1158/1078-0432.CCR-16-0597
67. Siegers GM, Dhamko H, Wang XH, Mathieson AM, Kosaka Y, Felizardo TC, et al. Human V $\delta$ 1  $\gamma\delta$  T cells expanded from peripheral blood exhibit specific cytotoxicity against B-cell chronic lymphocytic leukemia-derived cells. *Cytotherapy* (2011) 13:753–64. doi: 10.3109/14653249.2011.553595
68. Landin AM, Cox C, Yu B, Bejanyan N, Davila M, Kelley L. Expansion and enrichment of gamma-delta ( $\gamma\delta$ ) t cells from apheresed human product. *J Vis Exp* (2021) 2021:1–16. doi: 10.3791/62622
69. Choi H, Lee Y, Hur G, Lee S-E, Cho H-I, Sohn H-J, et al.  $\gamma\delta$  T cells cultured with artificial antigen-presenting cells and IL-2 show long-term proliferation and enhanced effector functions compared with  $\gamma\delta$  T cells cultured with only IL-2 after stimulation with zoledronic acid. *Cytotherapy* (2021) 23:908–17. doi: 10.1016/j.jcyt.2021.06.002
70. Zakeri N, Hall A, Swadling L, Pallett LJ, Schmidt NM, Diniz MO, et al. Characterisation and induction of tissue-resident gamma delta T-cells to target hepatocellular carcinoma. *Nat Commun* (2022) 13:1–16. doi: 10.1038/s41467-022-29012-1
71. Makkouk A, Yang XC, Barca T, Lucas A, Turkoz M, Wong JTS, et al. Off-the-shelf V $\delta$ 1 gamma delta T cells engineered with glypican-3 (GPC-3)-specific chimeric antigen receptor (CAR) and soluble IL-15 display robust antitumor efficacy against hepatocellular carcinoma. *J Immunother Cancer* (2021) 9(12). doi: 10.1136/jitc-2021-003441
72. Zhou J, Kang N, Cui L, Ba D, He W. Anti- $\gamma\delta$  TCR antibody-expanded  $\gamma\delta$  T cells: A better choice for the adoptive immunotherapy of lymphoid Malignancies. *Cell Mol Immunol* (2012) 9:34–44. doi: 10.1038/cmi.2011.16
73. de Waard AA, Verkerk T, Hoefakker K, van der Steen DM, Jongsma MLM, Melamed Kadosh D, et al. Healthy cells functionally present TAP-independent SSR1 peptides: implications for selection of clinically relevant antigens. *iScience* (2021) 24(2). doi: 10.1016/j.isci.2021.102051
74. Xiao L, Chen C, Li Z, Zhu S, Tay JC, Zhang X, et al. Large-scale expansion of V $\gamma$ 9V $\delta$ 2 T cells with engineered K562 feeder cells in G-Rex vessels and their use as chimeric antigen receptor–modified effector cells. *Cytotherapy* (2018) 20:420–35. doi: 10.1016/j.jcyt.2017.12.014
75. Dokouhaki P, Han M, Joe B, Li M, Johnston MR, Tsao M-S, et al. Adoptive immunotherapy of cancer using ex vivo expanded human gammadelta T cells: A new approach. *Cancer Lett* (2010) 297:126–36. doi: 10.1016/j.canlet.2010.05.005
76. Berglund S, Gaballa A, Sawasorn P, Sundberg B, Uhlin M. Expansion of gammadelta T cells from cord blood: A therapeutical possibility. *Stem Cells Int* (2018) 2018. doi: 10.1155/2018/8529104
77. Boucher JC, Yu B, Li G, Shrestha B, Sallman D, Landin AM, et al. Large scale ex vivo expansion of  $\gamma\delta$  T cells using artificial antigen-presenting cells. *J Immunother* (2023) 46:5–13. doi: 10.1097/CJI.0000000000000445
78. Nörenberg J, Jaksó P, Barakonyi A. Gamma/delta T cells in the course of healthy human pregnancy: cytotoxic potential and the tendency of CD8 expression make CD56 +  $\gamma\delta$ T cells a unique lymphocyte subset. *Front Immunol* (2021) 11:1–14. doi: 10.3389/fimmu.2020.596489
79. Holmen Olofsson G, Pedersen SR, Aehnlich P, Svane IM, Idorn M, thor Straten P. The capacity of CD4+ V $\gamma$ 9V $\delta$ 2 T cells to kill cancer cells correlates with co-expression of CD56. *Cytotherapy* (2021) 23:582–9. doi: 10.1016/j.jcyt.2021.02.003
80. Kadivar M, Petersson J, Svensson L, Marsal J. CD8 $\alpha\beta$ +  $\gamma\delta$  T cells: A novel T cell subset with a potential role in inflammatory bowel disease. *J Immunol* (2016) 197:4584–92. doi: 10.4049/jimmunol.1601146
81. Kozbor D, Trinchieri G, Monos DS, Isobe M, Russo G, Haney JA, et al. CD8+ T lymphocytes recognize tetanus toxoid in an MHC-restricted fashion. *J Exp Med* (1989) 169:1847–51. doi: 10.1084/jem.169.5.1847
82. Garcillán B, Marin AVM, Jiménez-Reinoso A, Briones AC, Muñoz-Ruiz M, García-León MJ, et al.  $\gamma\delta$  T lymphocytes in the diagnosis of human T cell receptor immunodeficiencies. *Front Immunol* (2015) 6:1–4. doi: 10.3389/fimmu.2015.00020
83. Siegers GM, Ribot EJ, Keating A, Foster PJ. Extensive expansion of primary human gamma delta T cells generates cytotoxic effector memory cells that can be labeled with Feraheme for cellular MRI. *Cancer Immunol Immunother* (2013) 62:571–83. doi: 10.1007/s00262-012-1353-y
84. Cho H-W, Kim S-Y, Sohn D-H, Lee M-J, Park M-Y, Sohn H-J, et al. Triple costimulation via CD80, 4-1BB, and CD83 ligand elicits the long-term growth of V $\gamma$ 9V $\delta$ 2 T cells in low levels of IL-2. *J Leukoc Biol* (2016) 99:521–9. doi: 10.1189/jlb.1HI0814-409RR
85. Van Bergen CAM, Van Luxemburg-Heijs SAP, De Wreede LC, Eefting M, Von Dem Borne PA, Van Balen P, et al. Selective graft-versus-leukemia depends on magnitude and diversity of the alloreactive T cell response. *J Clin Invest* (2017) 127:517–29. doi: 10.1172/JCI86175
86. Spaapen RM, De Kort RAL, Van Den Oudenalder K, Van Elk M, Bloem AC, Lokhorst HM, et al. Rapid identification of clinical relevant minor histocompatibility antigens via genome-wide zygosity-genotype correlation analysis. *Clin Cancer Res* (2009) 15:7137–43. doi: 10.1158/1078-0432.CCR-09-1914
87. de Vries NL, van de Haar J, Veninga V, Chalabi M, Ijsselstein ME, van der Ploeg M, et al.  $\gamma\delta$  T cells are effectors of immunotherapy in cancers with HLA class I defects. *Nature* (2023) 613:743–50. doi: 10.1038/s41586-022-05593-1
88. Chabab G, Barjon C, Bonnefoy N, Lafont V. Pro-tumor  $\gamma\delta$  T cells in human cancer: polarization, mechanisms of action, and implications for therapy. *Front Immunol* (2020) 11:1–12. doi: 10.3389/fimmu.2020.02186
89. Donia M, Ellebaek E, Andersen MH, Straten PT, Svane IM. Analysis of V $\delta$ 1 T cells in clinical grade melanoma-infiltrating lymphocytes. *Oncoimmunology* (2012) 1:1297–304. doi: 10.4161/onci.21659
90. Mikulak J, Oriolo F, Bruni E, Roberto A, Colombo FS, Villa A, et al. NKp46-expressing human gut-resident intraepithelial V $\delta$ 1 T cell subpopulation exhibits high antitumor activity against colorectal cancer. *JCI Insight* (2019) 4:1–19. doi: 10.1172/jci.insight.125884
91. Peng G, Wang HY, Peng W, Kিনিয়া Y, Seo KH, Wang RF. Tumor-infiltrating  $\gamma\delta$  T cells suppress T and dendritic cell function via mechanisms controlled by a unique toll-like receptor signaling pathway. *Immunity* (2007) 27:334–48. doi: 10.1016/j.immuni.2007.05.020
92. Wu P, Wu D, Ni C, Ye J, Chen W, Hu G, et al.  $\gamma\delta$ T17 cells promote the accumulation and expansion of myeloid-derived suppressor cells in human colorectal cancer. *Immunity* (2014) 40:785–800. doi: 10.1016/j.immuni.2014.03.013
93. Nishimoto KP, Barca T, Azameera A, Makkouk A, Romero JM, Bai L, et al. Allogeneic CD20-targeted  $\gamma\delta$  T cells exhibit innate and adaptive antitumor activities in preclinical B-cell lymphoma models. *Clin Transl Immunol* (2022) 11:e1373. doi: 10.1002/cti2.1373
94. Rozenbaum M, Meir A, Aharony Y, Itzhaki O, Schachter J, Bank I, et al. Gamma-delta CAR-T cells show CAR-directed and independent activity against leukemia. *Front Immunol* (2020) 11:1347. doi: 10.3389/fimmu.2020.01347